ΠΑΝΕΠΙΣΤΗΜΙΟ ΙΩΑΝΝΙΝΩΝ
ΤΜΗΜΑ ΜΑΘΗΜΑΤΙΚΩΝ

Μαρία Ελένη Παυλίδη

ΓΡΑΜΜΙΚΕΣ ΑΠΕΙΚΟΝΙΣΕΙΣ ΓΡΑΦΗΜΑΤΩΝ ΠΡΟΧΩΡΗΜΕΝΩΝ ΔΟΜΩΝ ΔΕΔΟΜΕΝΩΝ

ΜΕΤΑΠΤΥΧΙΑΚΗ ΔΙΑΤΡΙΒΗ

Ιωάννινα, 2023

UNIVERSITY OF IOANNINA

Department of Mathematics

Maria Eleni Pavlidi

Linear Graphs Layouts of Advanced Data Structures

Master's Thesis

Ioannina, 2023

Αφιερώνεται στην μητέρα μου.

Η παρούσα Μεταπτυχιακή Διατριβή εκπονήθηκε στο πλαίσιο των σπουδών για την απόκτηση του Μεταπτυχιακού Διπλώματος Ειδίκευσης στα Εφαρμοσμένα Μαθηματικά και Πληροφορικής, που απονέμει το Τμήμα Μαθηματικών του Πανεπιστημίου Ιωαννίνων.

Εγκρίθηκε την 06/07/2023 από την εξεταστική επιτροπή:

Ονοματεπώνυμο	**Βαθμίδα**
Μιχαήλ Μπέκος	Επίκουρος Καθηγητής
Χάρης Παπαδόπουλος	Αναπληρωτής Καθηγητής
Αντώνιος Συμβώνης	Καθηγητής

ΥΠΕΥΘΥΝΗ ΔΗΛΩΣΗ

"Δηλώνω υπεύθυνα ότι η παρούσα διατριβή εκπονήθηκε κάτω από τους διεθνείς ηθικούς και ακαδημαϊκούς κανόνες δεοντολογίας και προστασίας της πνευματικής ιδιοκτησίας. Σύμφωνα με τους κανόνες αυτούς, δεν έχω προβεί σε ιδιοποίηση ξένου επιστημονικού έργου και έχω πλήρως αναφέρει τις πηγές που χρησιμοποίησα στην εργασία αυτή."

Μαρία Ελένη Παυλίδη

Ευχαριστιες

Με την ολοκλήρωση της μεταπτυχιακής διατριβής μου, θα ήθελα να απευθύνω ένα ολόψυχο ευχαριστώ σε όσους στάθηκαν δίπλα μου σ' αυτή την προσπάθεια και με βοήθησαν να τη φέρω εις πέρας.

Πρώτον απ' όλους θα ήθελα να ευχαριστήσω τον επιβλέποντά μου κ. Μιχαήλ Μπέκο, Επίκουρο Καθηγητή του Πανεπιστημίου Ιωαννίνων, για την συνεχή υποστήριξή του και την καθοδήγησή του. Θα ήθελα επίσης, να τον ευχαριστήσω για τα εποικοδομητικά σχόλια και προτάσεις για την βελτίωση της διατρίβης. Επιπλέον, θα ήθελα να ευχαριστήσω τον κ. Michael Kaufman, Καθηγητή του Πανεπιστημίου του Tübingen, για τις συμβουλές και τα βοηθητικά σχόλια πάνω στην διατριβή.

Τέλος, ένα πολύ μεγάλο, ευχαριστώ στους δικούς μου ανθρώπους, που χωρίς την αγάπη και τη συμπαράστασή τους, η εκπόνηση και η ολοκλήρωση της διατριβής μου δε θα ήταν ποτέ δυνατή.

Περιληψη

Διάφορες γραμμικές απεικονίσεις γραφημάτων μπορούν να επιτευχθούν αξιοποιώντας γνωστές δομές δεδομένων, με τις διατάξεις στοίβας και ουράς να είναι οι πλέον δημοφιλής. Στόχος μας είναι να καθορίσουμε μια διάταξη των κορυφών και μια ανάθεση των ακμών σε *σελίδες* που επιτρέπουν στη δομή δεδομένων να επεξεργαστεί τις κορυφές-άκρες των ακμών κατά την καθορισμένη διάταξη.

Η παρούσα διατριβή εξετάζει τις rique απεικονίσεις γραφημάτων, οι οποίες προκύπτουν από την περιορισμένη-εισόδου διπλοουράς, γνωστή στην βιβλιογραφία επίσης ως rique. Η έρευνά μας επικεντρώνεται σε πλήρη γραφήματα και πλήρη διμερή γραφήματα, όπου παρουσιάζουμε φράγματα για τον ελάχιστο αριθμό σελίδων που απαιτούνται για οποιαδήποτε γραμμική απεικόνιση rique ενός δεδομένου γραφήματος. Στη μεταπτυχιακή αυτή διατριβή, βελτιώνουμε το υπάρχον άνω φράγμα για το πλήρες γράφημα K_n από $\lceil \frac{n}{3} \rceil$ σε $\lfloor \frac{n-1}{3} \rfloor$, και παρουσιάζουμε ένα νέο άνω φράγμα $\lfloor \frac{n-1}{2} \rfloor - 1$ για το πλήρες διμέρες γράφημα $K_{n,n}$.

Τέλος, εισαγάγουμε μια μοντελοποίηση βασισμένη σε SAT για τον υπολογισμό γραμμικών απεικονίσεων rique για δοθέντα γραφήματα. Επιβεβαιώνουμε την αποτελεσματικότητα της προσέγγισής μας υπολογίζοντας τον ελάχιστο αριθμό σελίδων που απαιτούνται σε γραμμικές απεικονίσεις rique γραφημάτων που είναι γνωστά στη βιβλιογραφία.

Abstract

Various linear graph layouts can be achieved by leveraging familiar data structures, with stack and queue layouts being the most prominent examples. The objective in this context is to determine a vertex order and an edge-partitioning into *pages* that allow the data structure to process the endpoints of the edges in the specified order.

This thesis examines rique layouts of graphs, which are obtained by utilizing the restricted-input double-ended queue, also known as rique. Our research focuses on complete graphs and complete bipartite graphs, where we present bounds on their rique numbers, where the rique number represents the minimum number of pages needed for any rique layout of a given graph. We improve the existing upper bound for the complete graph K_n from $\lceil \frac{n}{3} \rceil$ to $\lfloor \frac{n-1}{3} \rfloor$, and we introduce a new upper bound of $\lfloor \frac{n-1}{2} \rfloor - 1$ for the complete bipartite graph $K_{n,n}$. Finally, we propose a SAT-based formulation to compute the rique number of various graphs. We confirm the effectiveness of our approach by implementing it and by calculating the rique number of various graphs that are named in the literature.

Contents

CHAPTER 1

Introduction

Linear layouts of graphs form an important aspect in different contexts including Graph Theory and Graph Drawing. In a linear layout, the vertices of a graph are ordered based on a $\prec$. Typically, a *vertex order* $\prec$ of a graph G is a total order of its vertices, such that for any two vertices u and v of G, $u \prec v$ if and only if u precedes v in the order. To further ease a presentation, we write $[u_1, \ldots, u_k]$ if and only if $u_i \prec u_{i+1}$ for all $1 \leq i \leq k-1$. The linear layouts that we consider in this thesis are of the following type.

Definition 1.1. *Given a data structure D, a graph G admits a* D-layout *with* k-pages *if and only if there is a linear order $\prec$ of the vertices of G and a partition of its edges into k so-called pages such that the following hold. The data structure D is processing each edge (u, v) of G in the same page, by inserting (u, v) in D at u and removing it at v.*

Adopting a particular data structure D, one seeks to find the minimum number of pages required to construct a D-layout. In this aspect, D-layouts have naturally been leveraged to estimate the power of the respective data structures as a mean for representing graphs; in particular when D is a stack or a queue (for a wealth of other applications, e.g., to VLSI design and Graph Drawing, refer to [14]). In the linear layouts that we will consider, the data structure D will be either stack, queue, deque, or rique.

1.1 Stack layouts

If in Definition 1.1 the data structure D is a stack then the corresponding linear layouts are called *stack layouts* (also known as *book embeddings*). Stack layouts were first introduced in 1973 by Ollman [27] and over the years several remarkable results have been published in the literature [12, 22, 24, 25, 36].

In a stack, insertions, and removals occur only at the head of it. The *stack number* of a graph (a.k.a. *book thickness* or *page number* in the literature) is the minimum number of pages (called *stacks*) required in any of the stack layouts of the graph.

One can equivalently define a stack in a stack layout as follows. Let F be a set of $k \geq 2$ pairwise independent edges (u_i, v_i) of G, that is, $F = \{(u_i, v_i);\ i = 1, \ldots, k\}$. The edges of F form a *k-twist*, if the order of the vertices is $[u_1, \ldots, u_k, v_1, \ldots, v_k]$; see Fig. 1.1. Two independent edges (u_1, v_1) and (u_2, v_2) that form a 2-twist are commonly referred to as *crossing*. In this sense, a *stack* is a set of pairwise non-crossing edges in $\prec$.

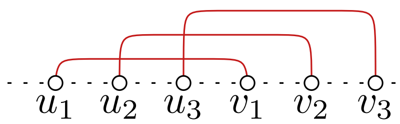

Figure 1.1: Illustration of a 3-twist

The corresponding problems are classified into two categories based on whether the graph is planar or non-planar. It is known that the stack number of the complete graph K_n is $\lceil \frac{n}{2} \rceil$ [9]. The stack number of outerplanar graphs is exactly 1 [9]. If a graph is sub-Hamiltonian, its stack number is at most 2 [9] while for non-sub-Hamiltonian planar graphs, Yannakakis has proved that their stack number is at most 4 [35, 36] which was recently to be worst case optimal [7, 37].

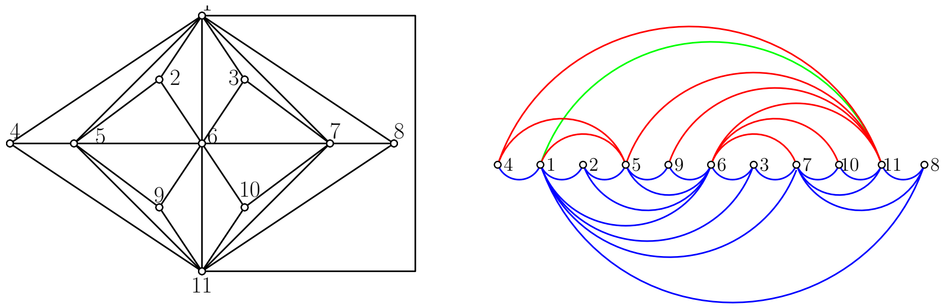

(a) (b)

Figure 1.2: Illustration of: (a) the Goldner Harary graph, and (b) a stack layout of its, where the first stack is formed by the red edges, the second stack is formed by the blue edges and the third page consists of the green edge.

Fig. 1.2 shows an example of a stack layout of the Goldner-Harary graph, which is an undirected graph with 11 vertices and 27 edges. It is named after A. Goldner and F. Harary, who proved in 1975 that this graph is the smallest non-Hamiltonian maximal planar graph [20]. This implies that the stack number of this graph is at least 3 while Fig. 1.2b shows that 3 stacks are sufficient.

1.2 Queue layouts

If in Definition 1.1 the data structure D is a *queue*, then the corresponding linear layouts are called *queue layouts*; recall that, in a queue, insertions occur at the head and removals occur at the tail of it. Queue layouts were introduced by Heath and Rosenberg in 1992 [9]. The *queue number* of a graph is the minimum of pages (called *queues*) required in any of the queue layouts of the graph.

Equivalently, we can define a queue in a queue layout as follows. Let F be a set of $k \geq 2$ pairwise independent edges (u_i, v_i) of G, that is, $F = \{(u_i, v_i);\ i = 1, \ldots, k\}$. If the order of F is $[u_1, \ldots, u_k, v_k, \ldots, v_1]$, then we say that the edges of F form a *k-rainbow*; see Fig. 1.3. Two independent edges (u_1, v_1) and (u_2, v_2) that form a 2-rainbow are commonly referred to as *nested*. In this sense, a *queue* is a set of pairwise non-nested edges in $\prec$. For an example of a queue layout, see Fig. 1.4, which shows that 2 queues are sufficient for a queue layout of the Goldner Harary graph.

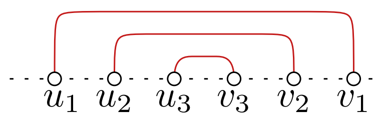

Figure 1.3: Illustration of a 3-rainbow

Applications of queue layouts include Graph Drawing [34, 19, 13], matrix computations [28] etc. It has been proven that the queue number of the complete graph K_n is $\lfloor \frac{n}{2} \rfloor$ [23]. Other known results are that the trees admit 1-queue layouts [22], outerplanar graphs admit 2-queue layouts [22], series-paralleled graphs admit queue layouts with at most 3-queues [29], and planar 3-trees with at most 5 [1]. In relation to stack layouts, it was recently shown that the stack number of a graph cannot always be bounded by its corresponding queue number [11], resolving a long-standing open question by

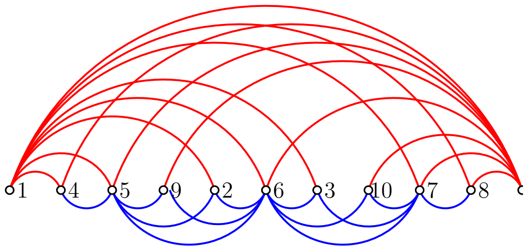

Figure 1.4: Illustration of a queue layout of Fig. 1.2a, where the first page is formed by the red edges and the second page is formed by the blue edges.

Heath, Leighton, and Rosenberg [22]; the other direction is still unknown.

1.3 Deque layouts

A data structure that generalizes both the stack and the queue is the so-called *double-ended queue* or *deque*, for short. A deque allows insertions and removals at both the head and the tail of the data structure. If in Definition 1.1 the data structure D is a *deque*, then the corresponding linear layouts are called *deque layouts*. Even though there exist many results for both stack and queue layouts, for deque layouts the corresponding literature is significantly reduced. Deque layouts were first introduced by Auer et al [3], who proved that a graph admits a 1-deque layout if and only if it is a spanning subgraph of a planar graph with a Hamiltonian path. Note that the *deque number* of a graph (that is, the minimum number of deques required by any of the deque layouts of the graph) has not been explicitly studied so far in the literature as a graph parameter. However, from the characterization by Auer et al. one can easily deduce the following.

Observation 1.1 (Auer et al. [3]). *The deque number of a graph is at most half of its stack number.*

Note that the queue number is also a trivial upper bound on the deque number of a graph. Observation 1.1, however, immediately implies improved upper bounds on the deque number of several graph classes, e.g., the deque-number of the complete graph K_n is at most $\lceil \frac{n}{4} \rceil$ [9], of the complete bipartite graph $K_{n.n}$ is at most $\lceil \frac{\lfloor 2n/3 \rfloor + 1}{2} \rceil$ [16], while of the treewidth-k graphs is at most $\lceil \frac{k+1}{2} \rceil$ [18]. Also, since there exist maximal planar graphs that do not have a Hamiltonian path (e.g., the n-vertex ones with an independent set of size greater than $\frac{n}{2}+2$), it follows by a well-known result by Yannakakis [36] that the deque number of planar graphs is 2; see also [7, 37].

Another consequence of Observation 1.1 is that deque layouts cannot be characterized by means of forbidden patterns in the underlying linear order, as it is the case, e.g., for stack and queue layouts [23, 27]; the former do not allow two edges of the same page to cross, while in the latter no two edges of the same page nest. The reason for the lack of such a characterization for deque layouts is the fact that maximal planar graphs with a Hamiltonian path are the maximal graphs that admit 2-stack layouts and these layouts do not admit characterizations in terms of forbidden patterns in the underlying linear order [32].

In the absence of a forbidden pattern, a single deque is more difficult to be described. A relatively intuitive way to describe a deque is as follows; assume that the vertices of a graph are arranged on a horizontal line ℓ from left to right according to $\prec$ (say, w.l.o.g., equidistantly). Then, each edge (v_i, v_j) with $v_i \prec v_j$ can be represented:

(i) either as a semi-circle that is completely above or completely below ℓ connecting u_i and u_j,

(ii) or as two semi-circles on opposite sides of ℓ, one that starts at u_i and ends at a point p_{ij} of ℓ to the right of the last vertex of $\prec$ and one that starts at point p_{ij} and ends at u_j.

With these in mind, a deque is a set of edges each of which can be represented with one of the two types (i) or (ii) that avoids crossings (such a representation is called *cylindric* in [3]). For an example of a deque layout, see Fig. 1.6, which shows that 1-deque is sufficient for a deque layout of the Goldner Harary graph. Observe that, a deque further allows classifying the edges into four categories: head-head, tail-tail, head-tail, and tail-head.

- A *head-head* (*hh* for short) edge is a type-(i) edge drawn above ℓ (see the dark blue edge of Fig. 1.5).
- A *tail-tail* (*tt* for short) edge is a type-(i) edge drawn below ℓ (see the light blue edge of Fig. 1.5).
- A *head-tail* (*ht* for short) edge is a type-(ii) edge whose first part is above ℓ, while its second part is below ℓ (see the dark red edge of Fig. 1.5).

- A *tail-head* (*th* for short) edge is a type-(ii) edge whose first part is below ℓ, while its second part is above ℓ (see the light red edge of Fig. 1.5).

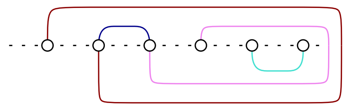

Figure 1.5: Illustration of a deque, where hh edge refers to blue, tt refers to light blue, ht refers to red, and th refers to light red

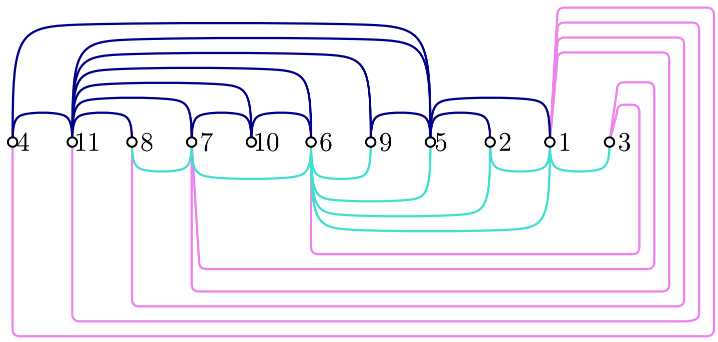

Figure 1.6: Illustration of a deque layout of the graph of Fig. 1.2a

1.4 Rique layouts

A special case of a deque is the so-called *restricted-input double-ended queue* or *rique* for short, which allows insertions only at the head and removals at both the head and tail of a data structure. Thus, if in Definition 1.1 the data structure is a *rique*, then the corresponding linear layouts are called *rique layouts* [4] and form a restricted case of the corresponding deque ones.

For a rique layout, a characterization in terms of forbidden patterns is possible [4]. A graph admits a 1-rique layout if and only if it admits a vertex order $\prec$ avoiding three edges (u_a, v_a), (u_b, v_b) and (u_c, v_c) such that $u_a \prec u_b \prec u_c \prec v_b \prec \{v_a, v_c\}$; see Fig. 1.7. A rique can also be equivalently defined as a deque without tail-tail and tail-head edges [4]. For an example of a rique layout, see Fig. 1.6, which shows that 2-riques are sufficient for a rique layout of the Goldner Harary graph.

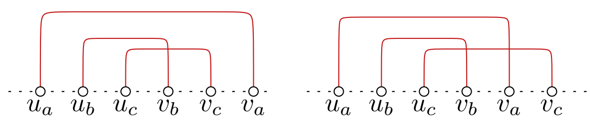

Figure 1.7: Illustration of the forbidden pattern of the rique layout

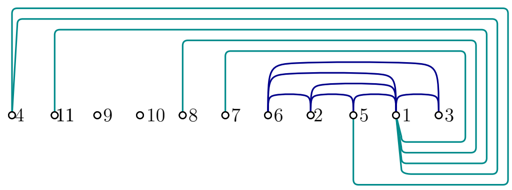

(a)

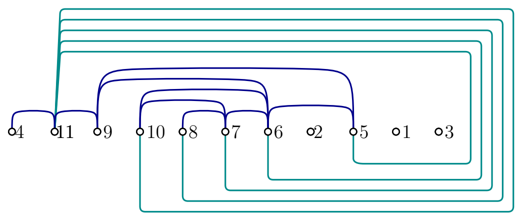

(b)

Figure 1.8: Illustration of a rique layout of the graph of Fig. 1.2a: (a) first page, (b) second page

1.5 Thesis Organization.

In this thesis, we improve the bound of the rique number of the complete graph K_n and present a new one for the complete bipartite graph $K_{n,n}$. More specifically, for the complete graph K_n our improvement is from $\lceil \frac{n}{3} \rceil$ [4] to $\lfloor \frac{n-1}{3} \rfloor$. For the complete bipartite graph $K_{n,n}$ our upper bound is $\lfloor \frac{n-1}{2} \rfloor - 1$. We complete our study by presenting the rique numbers of different graphs that are named in the literature.

This thesis is structured as follows:

- Chapter 2 focuses on the theoretical background of this thesis.

- Chapter 3 is devoted to the study of the rique number of the complete graph K_n.
- In Chapter 4 we study the rique number of the complete bipartite graph $K_{n,n}$.
- In Chapter 5, we introduce a SAT formulation for the problem of finding the rique number of a graph and we use an implementation of it to compute the rique numbers of different graphs that are named in the literature.
- Chapter 6 concludes this thesis with a discussion and a list of open problems raised by this work.

CHAPTER 2

Preliminaries

2.1 Complete and Bipartite Graphs

A graph G is defined as a pair of sets (V, E), where V is a finite set of *vertices* and E is a finite set of *edges* with $E \subseteq V \times V$. Every edge e of E has two endpoints. If these two endpoints of edge e are the vertices u and v, then we denote the edge e by (u, v). We further denote by $V(G)$ the set of vertices of G and by $E(G)$ the set of edges of G. The number of vertices of G is usually denoted by n while the number of its edges is usually denoted by m, i.e. $|V(G)| = n$ and $|E(G)| = m$.

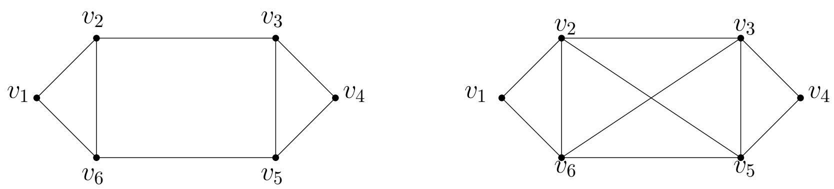

(a) A graph G

(b) A graph H

Figure 2.1: Illustration of two graphs G and H.

Two edges $e_i, e_j \in E(G)$ are called *adjacent* if they connect to the same vertex $u \in V(G)$. For a vertex $u \in V(G)$ we denote by $N_G(u)$, the set of the neighboring vertices of u. Correspondingly, two vertices $u_i, u_j \in V(G)$ are called *adjacent* or *neighboring* if they are the endpoints of the same edge $e \in E(G)$. Two edges that are not adjacent are called *independent*.

2.1.1 Complete Graphs

Definition 2.1. *Let G be a graph with $n \geq 1$ vertices and $m \geq 1$ edges. Graph G is called* complete *if and only if each pair of its vertices is connected by an edge.*

The complete graph with n vertices is denoted by K_n and has exactly $\frac{n(n-1)}{2}$ edges. Examples of complete graphs with different numbers of vertices are given in Fig. 2.2.

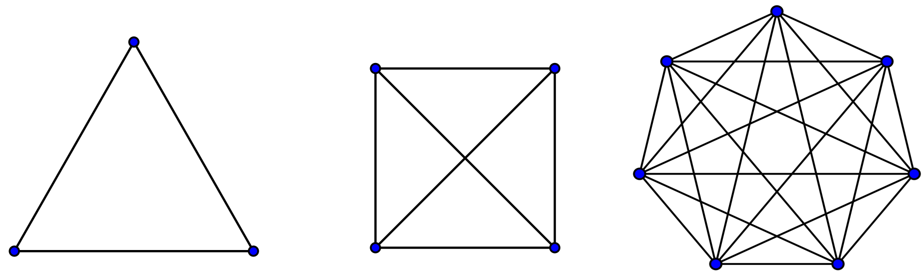

(a) K_3 (b) K_4 (c) K_7

Figure 2.2: Illustration of complete graphs with different numbers of vertices.

2.1.2 Bipartite Graphs

Definition 2.2. *Let G be a graph with $n \geq 1$ vertices and $m \geq 1$ edges. Graph G is called* bipartite *if and only if its vertex set $V(G)$ can be partitioned into two disjoint sets A and B, called* parts*, such that $V(G) = A \cup B$, $A \cap B = \emptyset$ and $E(G) \subseteq A \times B$. In other words, for every edge $(u, v) \in E(G)$, we have that $u \in A$ and $v \in B$.*

A bipartite graph G with parts A and B is denoted by $G = (A, B, E)$. A *complete bipartite* graph, also called *complete bigraph*, is a bipartite graph such that every vertex of one part is connected to every vertex of its other part, i.e., for every vertex $u \in A$ and for every vertex $v \in B$ the edge (u, v) belongs to $E(G)$. The complete bipartite graph is denoted by $K_{n,m}$, where $n = |A|$ and $m = |B|$, and has exactly nm edges. In this thesis, we assume that $n = m$. Examples of bipartite and complete bipartite graphs are given in Fig. 2.3.

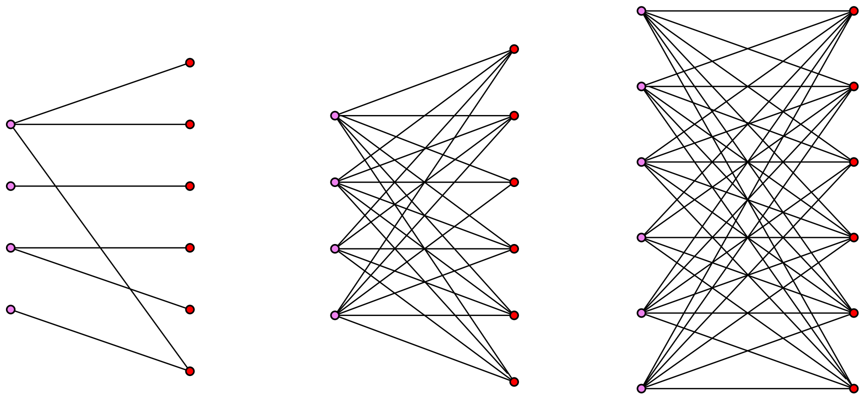

(a) (b) $K_{4,6}$ (c) $K_{6,6}$

Figure 2.3: Illustration of different bipartite graphs. The one of (a) is not complete, while the ones of (b) and (c) are.

2.2 A Short Introduction to SAT Formulations

A *propositional logic formula*, also called *Boolean expression* or SAT formula for short, is an expression that consists of different variables and operators, summarized in Table 2.1.

Function	Operator
AND	$\bigwedge$
OR	$\bigvee$
NOT	$\neg$
implies	$\rightarrow$
equivalence	$\leftrightarrow$

Table 2.1: Different operators appeared in a SAT formula.

Let F be a SAT formula. If F can be made `true` by assigning appropriate logic values to its variables, then F is said to be *satisfiable*. If no such assignment exists (that is, the formula is `false` for all possible variables assignments), then the formula is called *unsatisfiable*.

2.2.1 Linear Layouts and SAT Formulations

Bekos et al. [6] have already introduced and implemented SAT formulations for different types of linear layouts that are based on the original work [8]. The source code is available at `https://github.com/linear-layouts/SAT`. In the formulation, there exist three different types of variables, σ, ϕ, and χ with the following meanings.

- for a pair of vertices u and v, $\sigma(u, v)$ is `true`, if and only if u is to the left of v
- for an edge e and a page p, $\phi_p(e)$ is `true`, if and only if edge e is assigned to the page p , and
- for a pair of edges e and e',$\chi(e, e')$ is `true`, if and only if e and e' are assigned to the same page.

Therefore, the constructed formula has $O(n^2 + m^2 + pm)$ variables; see [8] for more details.

Especially, for the case where page p is a rique, Bekos et al. [4] introduce the following clause for each triplet of edges (u_a, v_a), (u_b, v_b) and (u_c, v_c) to express that the forbidden pattern $u_a \prec u_b \prec u_c \prec v_b \prec \{v_a, v_c\}$ does not occur at page p.

$$\sigma(u_a, u_b) \wedge \sigma(u_b, u_c) \wedge \sigma(u_c, v_b) \wedge \sigma(v_b, v_a) \wedge \sigma(v_b, v_c) \rightarrow$$
$$\neg(\phi_p(u_a, v_a) \wedge \phi_p(u_b, v_b) \wedge \phi_p(u_c, v_c))$$

In practice, we observed that the formulation above was inefficient. Rieger [30] also observed this issue for the more general case where p is a deque and introduced $4m$ variables to resolve it. More precisely, for each edge e and each x in $\{hh, ht, th, tt\}$ variable $\tau_p(e, x)$ has the following meaning.

$\tau_p(e, x)$ is `true`, if and only if the type of edge e at page p is x.

Rieger ensures that each edge has at least one of the allowed types, by introducing the following clause for each edge e:

$$\vee_{i=1}^{p}(\tau_i(e, hh) \vee \tau_i(e, ht) \vee \tau_i(e, th) \vee \tau_i(e, tt))$$

Using the variables above, Rieger introduces $O(m^2)$ clauses for each deque p to ensure that all edges in p form a cylindric layout. In Chapter 5 we describe how to adjust the formulation by Rieger in the case in which p is a rique.

2.3 Matrix Representations of Linear Layouts

For convenience, we represent their linear layouts as in [26]. Let $\prec$ be an order of the n vertices $v_1, \ldots, v_n$ of a graph G such that $v_1 \prec \cdots \prec v_n$. Then, each edge (v_i, v_j) of G with $i < j$ is mapped to point (i, j) of the $n \times n$ grid $H = [1, n] \times [1, n]$. A set of head-head edges corresponds to a set of monotonically decreasing paths on H [26], while a set of head-tail edges corresponds to monotonically increasing paths on H [2].

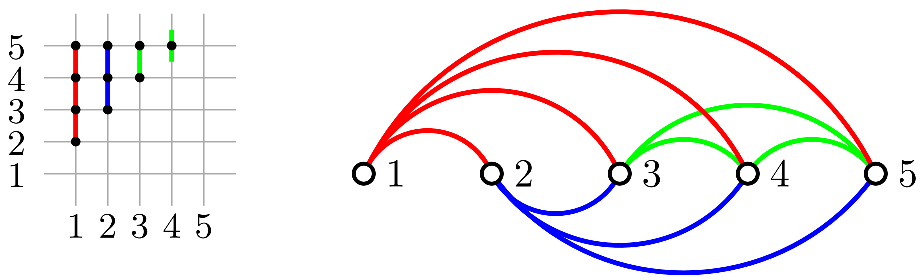

Figure 2.4: A stack layout of K_5 and its corresponding matrix representation.

CHAPTER 3

An Upper Bound on the Rique Number of Complete Graphs

In this section, we study the rique number of the complete graph K_n. To show a lower bound of $(1-\frac{\sqrt{2}}{2})(n-2)$, Bekos et al. [4] have used the following lemma.

Lemma 3.1 (Bekos et al. [4])**.** *A graph with n vertices admitting a rique layout with k pages has at most $(2n+2)k-k^2+(n-3)$ edges.*

The best-known upper bound on the rique number of K_n is $\lceil \frac{n}{3} \rceil$ [4]. In the next theorem, we improve this bound to $\lfloor \frac{n-1}{3} \rfloor$. Given a rique layout L and a set of edges E, we write E_x to denote that all edges of E are of type-x in L, where $x \in \{hh, ht\}$.

Theorem 3.1. *The rique-number of K_n is at most $\lfloor \frac{n-1}{3} \rfloor$.*

Proof. For the proof, we assume three cases for K_n, namely, $n \bmod 3 \in 0, 1, 2$. First, we assume $n \bmod 3 = 0$ and we prove that K_n admits a rique layout $\mathcal{L}$ with $\frac{n}{3}-1$ riques.

Page 1 of $\mathcal{L}$ contains the following $2n$ edges; see Fig. 3.1:

- $\{(v_1, v_j), j = 2, \ldots, n\}_{ht}$; dark red in Fig. 3.1,
- $\{(v_i, v_n), i = 2, \ldots, \frac{n}{3}\}_{ht}$; red in Fig. 3.1,
- $\{(v_{\frac{n}{3}}, v_j), j = \frac{n}{3} + 1, \ldots, \frac{2n}{3} + 1\}_{hh}$; light red in Fig. 3.1,
- $\{(v_{\frac{2n}{3}+1}, v_j), j = \frac{2n}{3} + 2, \ldots, n\}_{hh}$; blue in Fig. 3.1,
- $\{(v_{n-1}, v_n)\}_{hh}$; light blue in Fig. 3.1 .

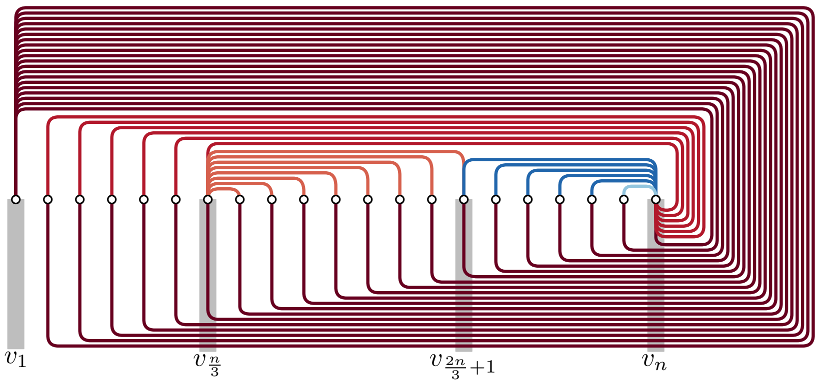

Figure 3.1: Page 1 of $\mathcal{L}$ when $n \bmod 3 = 0$.

Page 2 of $\mathcal{L}$ contains the following $2n-7$ edges:

- $\{(v_2, v_j), j = 3, \dots, n-1\}_{ht}$; dark red in Fig. 3.2,
- $\{(v_i, v_{n-1}), i = 3, \dots, \frac{n}{3}+1\}_{ht}$; red in Fig. 3.2,
- $\{(v_{\frac{n}{3}+1}, v_n)\}_{ht}$; orange in Fig. 3.2,
- $\{(v_{\frac{n}{3}+1}, v_j), j = \frac{n}{3}+2, \dots, \frac{2n}{3}\}_{hh}$; blue in Fig. 3.2,
- $\{(v_{\frac{2n}{3}}, v_j), j = \frac{2n}{3}+1, \dots, n\}_{hh}$; light blue in Fig. 3.2.

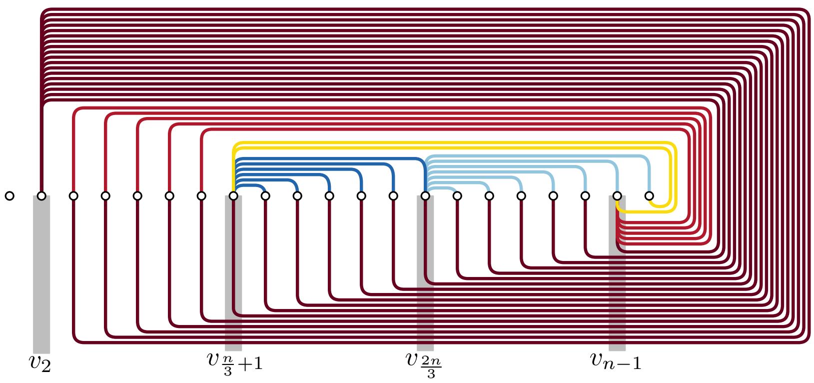

Figure 3.2: Page 2 of $\mathcal{L}$ when $n \bmod 3 = 0$.

Page 3 of $\mathcal{L}$ contains the following $2n-5$ edges:

- $\{(v_3, v_j), j = 4, \ldots, n-2\}_{ht}$; dark red in Fig. 3.3,
- $\{(v_i, v_{n-2}), i = 4, \ldots, \frac{n}{3}+1\}_{ht}$; red in Fig. 3.3,
- $\{(v_{\frac{2n}{3}+2}, v_j), j = n-2, \ldots, n\}_{ht}$; orange in Fig. 3.3,
- $\{(v_{\frac{n}{3}+1}, v_{\frac{2n}{3}+1})\}_{hh}$; blue in Fig. 3.3,
- $\{(v_{\frac{n}{3}+2}, v_j), j = \frac{2n}{3}-1, \frac{2n}{3}, \frac{2n}{3}+1\}_{hh}$; light blue in Fig. 3.3,
- $\{(v_{\frac{n}{3}+3}, v_j), j = \frac{n}{3}+4, \ldots, \frac{2n}{3}-1\}_{hh}$; pink in Fig. 3.3,
- $\{(v_{\frac{2n}{3}+2}, v_j), j = \frac{2n}{3}+3, \ldots, n-3\}_{hh}$; light red in Fig. 3.3,
- $\{(v_{n-3}, v_j), j = n-2, n-1, n\}_{hh}$; light orange in Fig. 3.3.

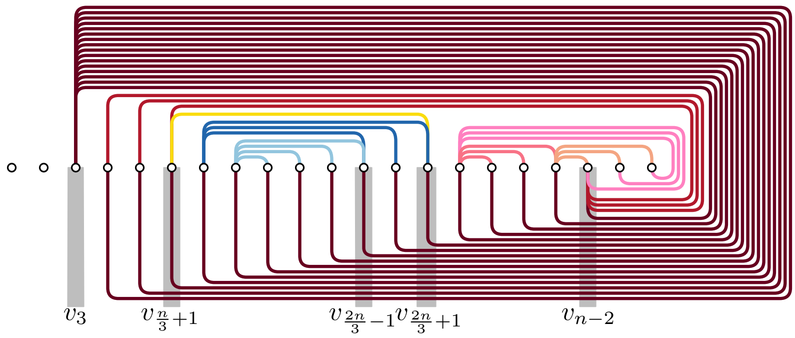

Figure 3.3: Page 3 of $\mathcal{L}$ when $n \bmod 3 = 0$.

For $p = 4, \ldots, \frac{n}{3} - 4$, page p of $\mathcal{L}$ contains the following $\frac{n}{3} - 2p + 3$ edges:

- $\{(v_p, v_j), j = p+1, \ldots, n-p+1\}_{ht}$; dark red in Fig. 3.4,
- $\{(v_i, v_j), i = p+1, \ldots \frac{n}{3}+1, j = n-p+1\}_{ht}$; red in Fig. 3.4,
- $\{(v_i, v_j), i = \frac{n}{3} + (p+1), j = n-p+1, \ldots, n\}_{ht}$; pink in Fig. 3.4,
- $\{(v_i, v_j), i = \frac{n}{3} + (p+1), j = \frac{2n}{3} + (p-2), \ldots, n-p\}_{hh}$; blue in Fig. 3.4,
- $\{(v_i, v_j), i = n-p+1, j = n-p, \ldots, n\}_{hh}$; light blue in Fig. 3.4,
- $\{(v_i, v_j), i = \frac{n}{3} + (p+2), j = \frac{n}{3} + (p+3), \ldots, \frac{2n}{3} + (p-2)\}_{hh}$; orange in Fig. 3.4.

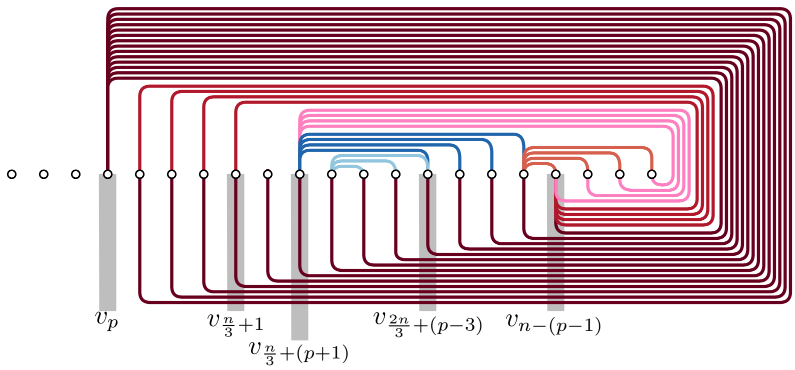

Figure 3.4: Page $p = 4, \ldots, \frac{n}{3} - 4$ of $\mathcal{L}$ when $n \bmod 3 = 0$.

Page $\frac{n}{3}-3$ of $\mathcal{L}$ contains the following $\frac{4n}{3}+6$ edges:

- $\{(v_{\frac{n}{3}-3}, v_j), j=\frac{n}{3}-2, \ldots, \frac{2n}{3}+4\}_{ht}$; dark red in Fig. 3.5,
- $\{(v_i, v_{\frac{2n}{3}+4}), i=\frac{n}{3}-2, \ldots, \frac{n}{3}+1\}_{ht}$; red in Fig. 3.5,
- $\{(v_{\frac{n}{3}+3}, v_j), j=\frac{2n}{3}+4, \ldots, n-1\}_{ht}$; light blue in Fig. 3.5,
- $\{(v_{\frac{2n}{3}+3}, v_j), j=n-1, n\}_{ht}$; pink in Fig. 3.5,
- $\{(v_{\frac{n}{3}+3}, v_j), j=\frac{2n}{3}, \ldots, \frac{2n}{3}+3\}_{hh}$; dark blue in Fig. 3.5,
- $\{(v_{\frac{n}{3}+4}, v_j), j=\frac{n}{3}+5, \ldots, \frac{2n}{3}\}_{hh}$; orange in Fig. 3.5,
- $\{(v_{\frac{2n}{3}+3}, v_j), j=\frac{2n}{3}+3, \ldots, n-2\}_{hh}$; red in Fig. 3.5,
- $\{(v_{n-2}, v_j), j=n-1, n\}_{hh}$; dark orange in Fig. 3.5.

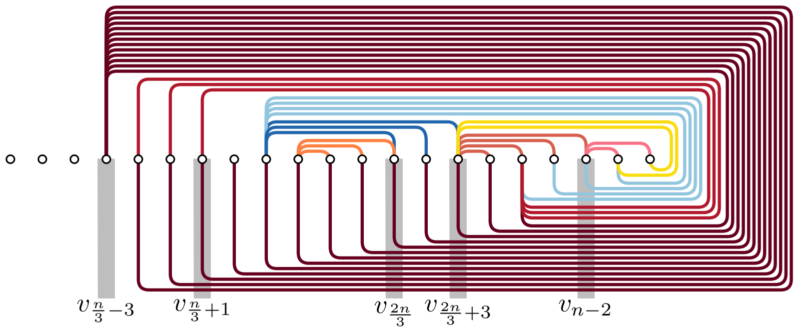

Figure 3.5: Page $\frac{n}{3}-3$ of $\mathcal{L}$ when $n \bmod 3 = 0$.

Page $\frac{n}{3}-2$ of $\mathcal{L}$ contains the following $\frac{4n}{3}+3$ edges:

- $\{(v_{\frac{n}{3}-2}, v_j), j = \frac{n}{3}-1, \ldots, \frac{2n}{3}+3\}_{ht}$; dark red in Fig. 3.6,
- $\{(v_i, v_{\frac{2n}{3}+3}), i = \frac{n}{3}-1, \ldots, \frac{n}{3}+1\}_{ht}$; red in Fig. 3.6,
- $\{(v_{\frac{n}{3}+2}, v_j), j = \frac{2n}{3}+3, \ldots, n\}_{ht}$; light red in Fig. 3.6,
- $\{(v_{\frac{n}{3}+3}, v_n)_{ht}$; pink in Fig. 3.6,
- $\{(v_{\frac{n}{3}+4}, v_j), j = \frac{2n}{3}+1, \ldots, n\}_{hh}$; dark orange in Fig. 3.6,
- $\{(v_{\frac{n}{3}+5}, v_j), j = \frac{n}{3}+6, \ldots, \frac{2n}{3}+1\}_{hh}$; orange in Fig. 3.6.

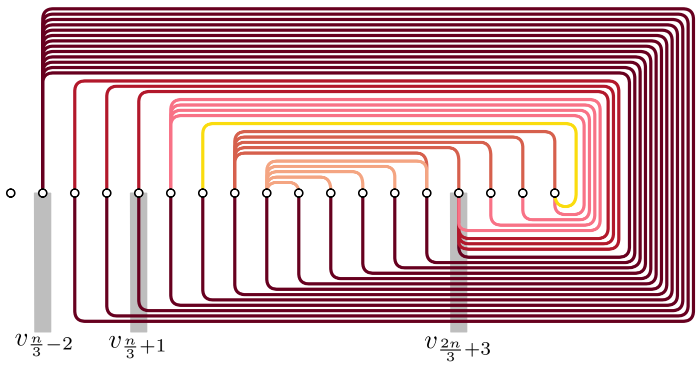

Figure 3.6: Page $\frac{n}{3}-2$ of $\mathcal{L}$ when $n \bmod 3 = 0$.

Page $\frac{n}{3}-1$ of $\mathcal{L}$ contains the following $n+9$ edges:

- $\{(v_{\frac{n}{3}-1}, v_j), j = \frac{n}{3}, \ldots, \frac{2n}{3}+2\}_{ht}$; dark red in Fig. 3.7,
- $\{(v_i, v_{\frac{2n}{3}+2}), i = \frac{n}{3}, \ldots, \frac{n}{3}+2\}_{ht}$;red in Fig. 3.7,
- $\{(v_{\frac{2n}{3}-2}, v_j), j = n-5, \ldots, n\}_{ht}$; light red in Fig. 3.7,
- $\{(v_{\frac{n}{3}+2}, v_j), j = \frac{n}{3}+3, \ldots, \frac{2n}{3}-2\}_{hh}$; orange in Fig. 3.7,
- $\{(v_{\frac{2n}{3}-1}, v_j), j = \frac{2n}{3}, \ldots, n\}_{hh}$; light orange in Fig. 3.7.

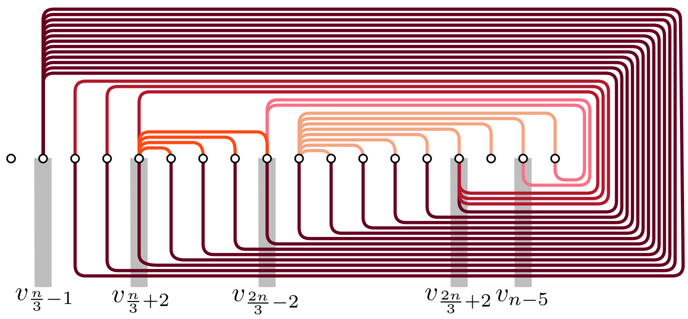

Figure 3.7: Page $\frac{n}{3}-1$ of $\mathcal{L}$ when $n \bmod 3 = 0$.

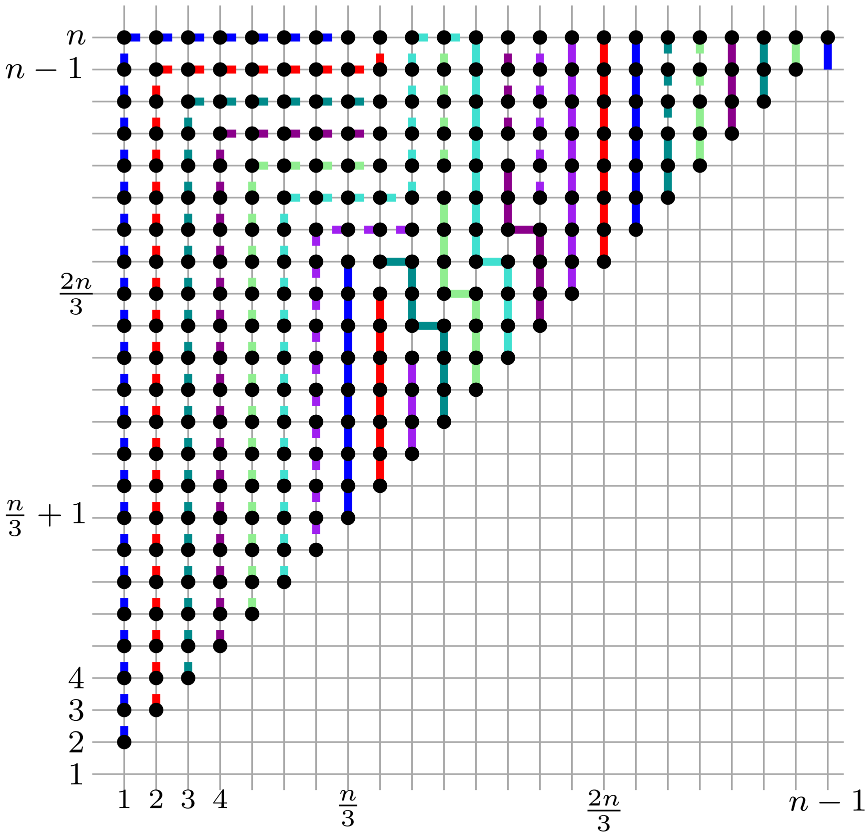

Figure 3.8: Illustration of the grid representation of a rique layout of K_n with $n \bmod 3 = 0$ in which paths of the same color correspond to the same rique. The points of the grid that are covered by a solid (dashed) path are head-head (head-tail, respectively). Here, the "special" edges are the first (blue), second (red), third (light green), $\frac{n}{3}-3$ (green), $\frac{n}{3}-2$ (light blue) and $\frac{n}{3}-1$ (purple)

Case 2: $n \bmod 3 = 1$. In this case, we show that the K_n admits a rique layout with $\lfloor \frac{n}{3} \rfloor$ riques. As in Case 1, our construction contains again “special” pages, namely, the ones in $\{1, 2, \lfloor \frac{n-1}{3} \rfloor\}$; blue, red and purple in Fig. 3.13. The remaining pages of $\mathcal{L}$ are uniform.

Page 1 of $\mathcal{L}$ contains the following $2n - 1$ edges:

- $\{(u_1, v_j), j = 2, \ldots, n\}_{ht}$; dark red in Fig. 3.9,
- $\{(u_i, v_n), i = 2, \ldots, \frac{n-1}{3} + 1\}_{ht}$; red in Fig. 3.9,
- $\{(u_{\frac{n-1}{3}+1}, v_j), j = \frac{n-1}{3} + 2, \ldots, \frac{2n-2}{3} + 1\}_{hh}$; light red in Fig. 3.9,
- $\{(u_{\frac{2n-2}{3}+1}, v_j), j = \frac{2n-2}{3} + 2, \ldots, n\}_{hh}$; blue in Fig. 3.9,
- $\{(u_{n-1}, v_n)\}_{hh}$; light blue in Fig. 3.9.

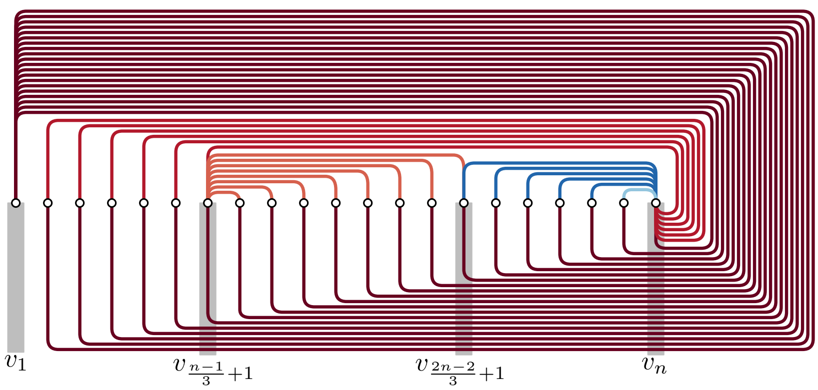

Figure 3.9: Page 1 of $\mathcal{L}$ when $n \bmod 3 = 1$.

Page 2 of $\mathcal{L}$ contains the following $2n-4$ edges:

- $\{(u_2, v_j), j = 3, \ldots, n-1\}_{ht}$; dark red in Fig. 3.10,
- $\{(u_i, v_{n-1}), i = 3, \ldots, \frac{n-1}{3}+1\}_{ht}$; red in Fig. 3.10,
- $\{(u_{\frac{n-1}{3}+2}, v_j), j = n-1, n\}_{ht}$; light red in Fig. 3.10,
- $\{(u_{\frac{n-1}{3}+2}, v_j), j = \frac{n-1}{3}+3 \ldots, n-2\}_{hh}$; blue in Fig. 3.10,
- $\{(u_{n-2}, v_j), j = n-1, n\}_{hh}$; light blue in Fig. 3.10.

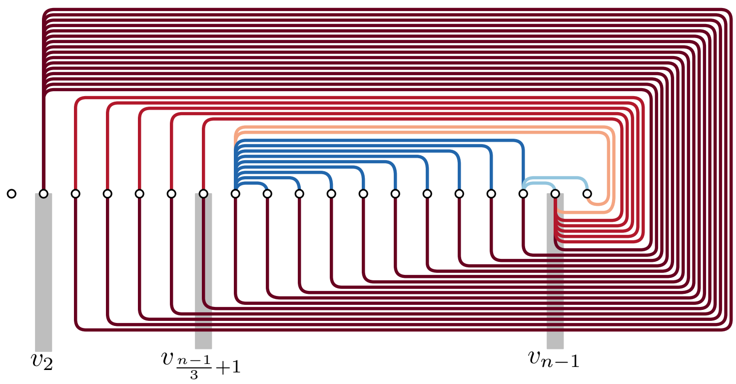

Figure 3.10: Page 2 of $\mathcal{L}$ when $n \bmod 3 = 1$.

For $p = 3, \ldots, \frac{n-1}{3} - 1$, page p of $\mathcal{L}$ contains the following $2n - 3p + 2$ edges:

- $\{(u_p, v_j), j = p+1, \ldots, n-p+1\}_{ht}$; dark red in Fig. 3.11,
- $\{(u_i, v_{n-p+1}), i = p+1, \ldots, \frac{n-1}{3} + 1\}_{ht}$; red in Fig. 3.11,
- $\{(u_{\frac{n-1}{3}+p}, v_j), j = n-p+1, \ldots, n\}_{ht}$; orange in Fig. 3.11,
- $\{(u_{\frac{n-1}{3}+p}, v_j), j = \frac{n-1}{3} + (p+1), \ldots, n-p\}_{hh}$; blue in Fig. 3.11,
- $\{(u_{n-p}, v_j), j = n-p+1, \ldots, n\}_{hh}$; light blue in Fig. 3.11.

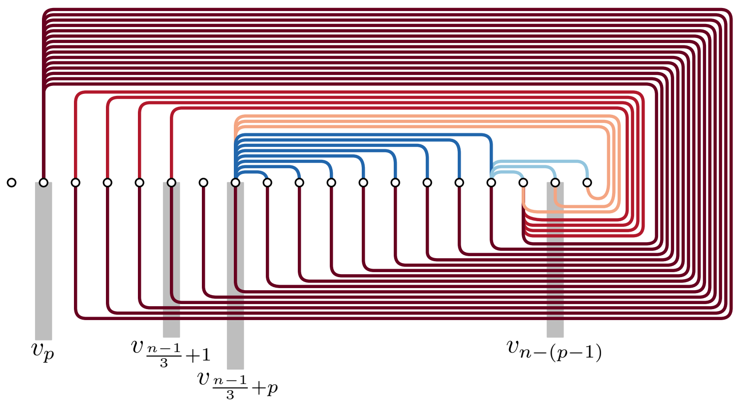

Figure 3.11: Page $p = 3, \ldots, \frac{n-1}{3} - 1$ of $\mathcal{L}$ when $n \bmod 3 = 1$.

Page $\lfloor \frac{n-1}{3} \rfloor$ of $\mathcal{L}$ contains the following $2(\frac{n-1}{3}) + 4$ edges:

- $\{(u_{\frac{n-1}{3}}, v_j), j = \frac{n-1}{3} + 1, \ldots, \frac{2n-2}{3} + 2)\}_{ht}$; dark red in Fig. 3.12,
- $\{(u_{\frac{n-1}{3}+1}, v_{\frac{2n-2}{3}+2}), \}_{ht}$; red in Fig. 3.12,
- $\{(u_{\frac{2n-2}{3}}, v_j), j = \frac{2n-2}{3} + 1, \ldots, n\}_{hh}$; orange in Fig. 3.12.

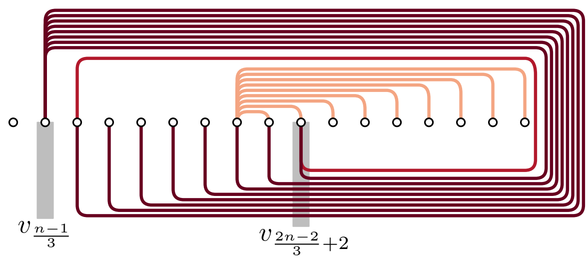

Figure 3.12: Page $\lfloor \frac{n-1}{3} \rfloor$ of $\mathcal{L}$ when $n \bmod 3 = 1$.

So, when $n \bmod 3 = 1$, $\mathcal{L}$ has $2n-1+2n-4+\sum_{p=3}^{\frac{n-1}{3}-1}(2n-3p+2)+2(\frac{n-1}{3})+4 = \frac{n(n-1)}{2}$ edges. Since no two edges have been assigned to the same rique and all edges in the same rique form a cylindric layout, it follows that the rique number of K_n is at most $\frac{n-1}{3}$ when $n \bmod 3 = 1$.

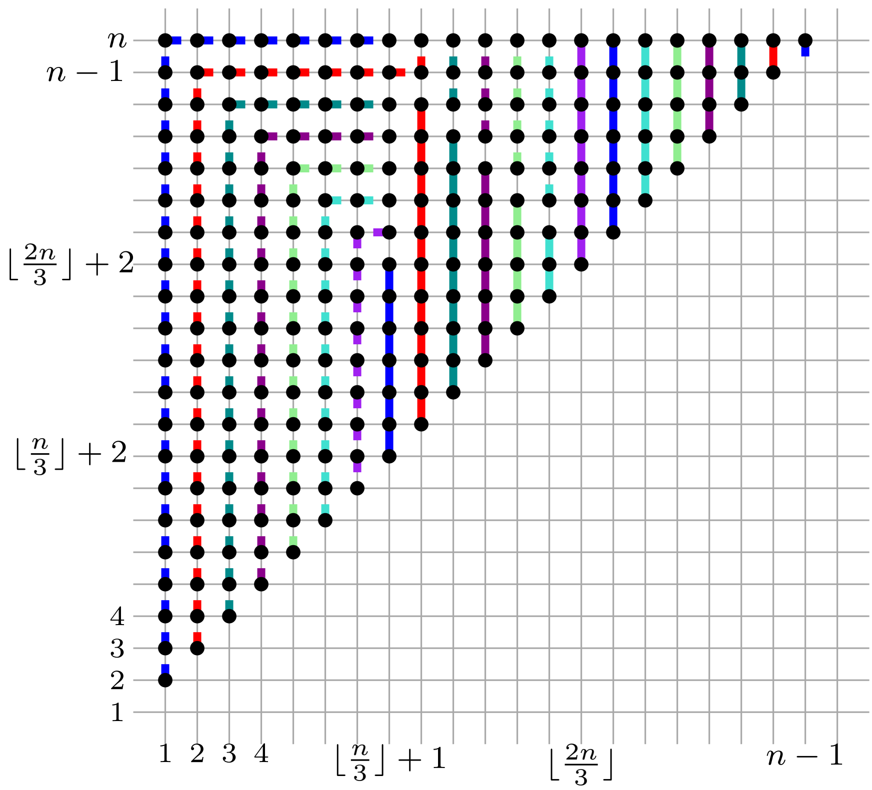

Figure 3.13: Illustration of the grid representation of a rique layout of K_n with $n \bmod 3 = 1$ in which paths of the same color correspond to the same rique. The points of the grid that are covered by a solid (dashed) path are head-head (head-tail, respectively). Here, the "special" edges are the first (blue), second (red), and the $\frac{n-1}{3}$ (purple).

Case 3: $n \bmod 3 = 2$. We continue with the case $n \bmod 3 = 2$. In this case, we show that the K_n admits a rique layout with $\lfloor \frac{n}{3} \rfloor$ riques. As with the previous two cases, our construction contains again "special" pages, namely, the ones in $\{1, 2\}$; blue and red in Fig. 3.17. The remaining pages of $\mathcal{L}$ are uniform.

Page 1 of $\mathcal{L}$ contains the following $2n$ edges:

- $\{(u_1, v_j), j = 2, \ldots, n\}_{ht}$; dark red in Fig. 3.14,
- $\{(u_i, v_n), i = 2, \ldots, \frac{n-2}{3} + 1\}_{ht}$; red in Fig. 3.14,
- $\{(u_{\frac{n-2}{3}+1}, v_j), j = \frac{n-2}{3} + 2, \ldots, \frac{2n-4}{3} + 2\}_{hh}$; light red in Fig. 3.14,
- $\{(u_{\frac{2n-4}{3}+2}, v_j), j = \frac{2n-4}{3} + 3, \ldots, n\}_{hh}$; blue in Fig. 3.14,
- $\{(u_{n-1}, v_n)\}_{hh}$; light blue in Fig. 3.14.

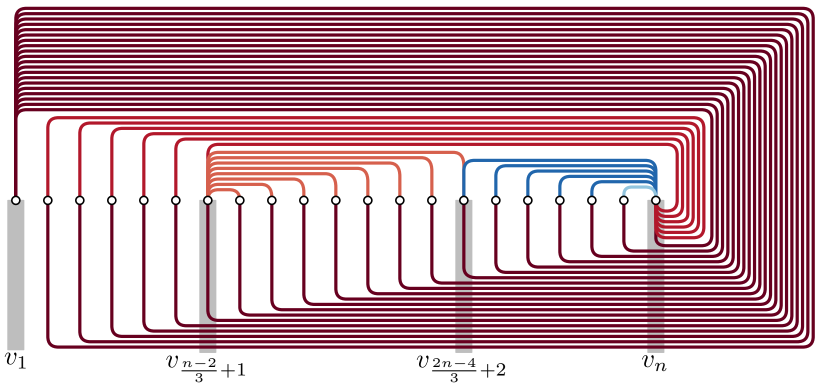

Figure 3.14: Page 1 of $\mathcal{L}$ when $n \bmod 3 = 2$.

Page 2 of $\mathcal{L}$ contains the following $2n - 4$ edges:

- $\{(u_2, v_j), j = 3, \ldots, n-1\}_{ht}$; dark red in Fig. 3.15,
- $\{(u_i, v_{n-1}), i = 3, \ldots, \frac{n-2}{3} + 2\}_{ht}$; red in Fig. 3.15,
- $\{(u_{\frac{n-2}{3}+2}, v_j), j = n-1, n\}_{ht}$; light red in Fig. 3.15,
- $\{(u_{\frac{n-2}{3}+2}, v_j), j = \frac{n-2}{3} + 3 \ldots, n-2\}_{hh}$; blue in Fig. 3.15,
- $\{(u_{n-2}, v_j), j = n-1, n\}_{hh}$; light blue in Fig. 3.15.

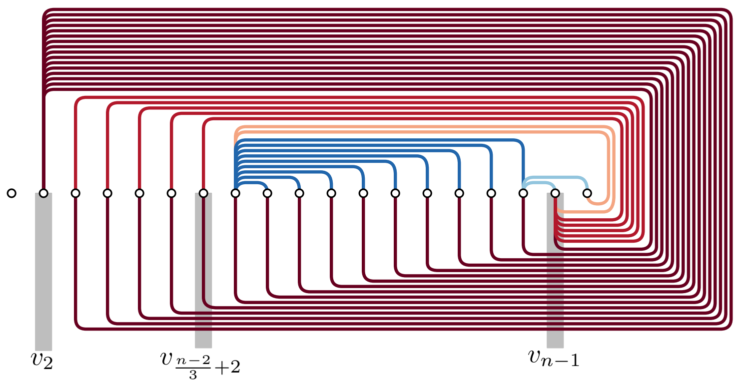

Figure 3.15: Page 2 of $\mathcal{L}$ when $n \bmod 3 = 2$.

For $p = 3, \dots, \frac{n-2}{3}$, page p of $\mathcal{L}$ contains the following $2n - 3p + 2$ edges:

- $\{(u_p, v_j), j = p + 1, \dots, n - p + 1\}_{ht}$; dark red in Fig. 3.16,
- $\{(u_i, v_{n-p+1}), i = p + 1, \dots, \frac{n-2}{3} + 1\}_{ht}$; red in Fig. 3.16,
- $\{(u_{\frac{n-2}{3}+p}, v_j), j = n - p + 1, \dots, n\}_{ht}$;light red in Fig. 3.16,
- $\{(u_{\frac{n-2}{3}+p}, v_j), j = \frac{n-2}{3} + (p + 1), \dots, n - p\}_{hh}$; blue in Fig. 3.16,
- $\{(u_{n-p}, v_j), j = n - p + 1, \dots, n\}_{hh}$; light blue in Fig. 3.16.

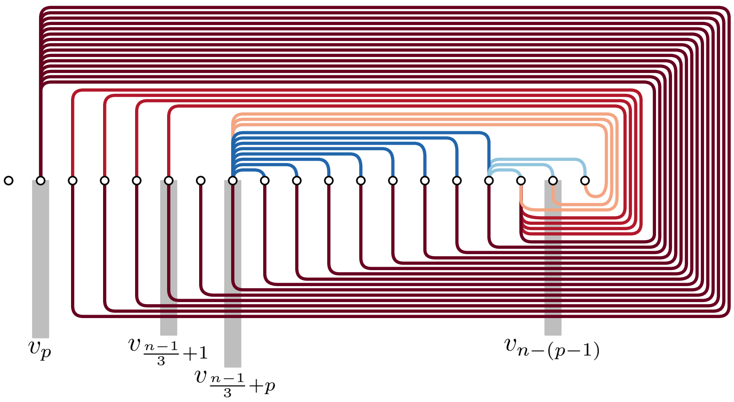

Figure 3.16: Page $p = 3, \dots, \frac{n-2}{3}$ of $\mathcal{L}$ when $n \bmod 3 = 2$.

So, in total $\mathcal{L}$ has $2n + 2n - 4 + \sum_{p=3}^{\frac{n-2}{3}}(2n - 3p + 2) = \frac{n(n-1)}{2}$ edges. Since no two edges have been assigned to the same rique and all edges in the same rique form a cylindric layout, it follows that the rique number of K_n is at most $\frac{n-2}{3}$ when $n \bmod 3 = 2$.

$\square$

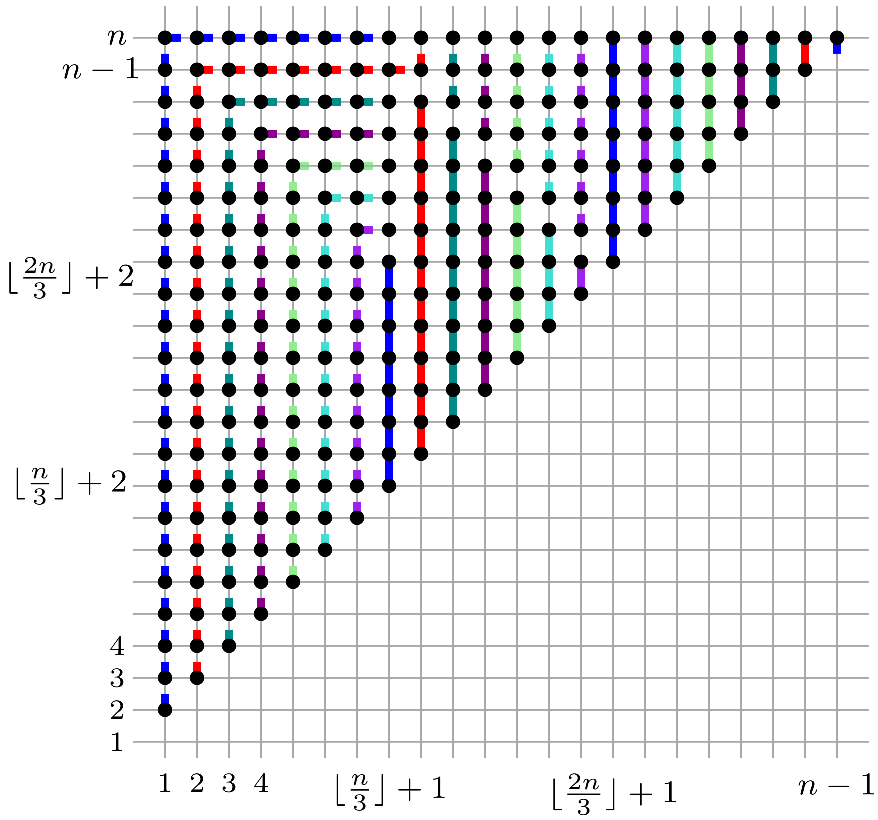

Figure 3.17: Illustration of the grid representation of a rique layout of K_n with $n \bmod 3 = 2$ in which paths of the same color correspond to the same rique. The points of the grid that are covered by a solid (dashed) path are head-head (head-tail, respectively). Here, the "special" edges are the first (blue), and the second (red).

CHAPTER 4

An Upper Bound on the Rique Number of Complete Bipartite Graphs

In this section, we study the rique number of the complete bipartite graph $K_{n,n}$. Let the two parts of $K_{n,n}$ be $A = \{a_1, \ldots, a_n\}$ and $B = \{b_1, \ldots, b_n\}$ with $|A| = |B| = n$. W.l.o.g., we also assume that in the computed layouts $a_1 \prec \ldots a_n$ and $b_1 \prec \cdots \prec b_n$ holds. As in Chapter 3, given a rique layout L and a set of edges E, we write E_x to denote that all edges of E are of type-x in L, where $x \in \{hh, ht\}$.

Theorem 4.1. *The rique-number of the complete bipartite graph $K_{n,n}$ is at most $\lfloor \frac{n-1}{2} \rfloor - 1$.*

Proof. For the proof, we assume two cases for $K_{n,n}$, one for the oss numbers ade one for the even ones. Given a rique layout L and a set of edges E, we write E_x to denote that all edges of E are of type-x in L, where $x \in \{hh, ht\}$.

First, we prove that $K_{n,n}$ with n odd, admits a rique layout $\mathcal{L}$ with $\lfloor \frac{n}{2} \rfloor - 1$ riques. We assume that for the two parts A and B of $K_{n,n}$, $a_1 \prec b_1 \prec a_2 \prec b_2 \prec \cdots \prec a_{\lfloor \frac{n}{2} \rfloor} \prec b_{\lfloor \frac{n}{2} \rfloor} \prec b_{\lceil \frac{n}{2} \rceil} \prec \cdots \prec b_n \prec a_{\lceil \frac{n}{2} \rceil} \prec \cdots \prec a_n$ holds in $\mathcal{L}$.

Page 1 of $\mathcal{L}$ contains the following 3n edges:

- $\{(a_1, b_j), j = 1, \ldots, n\}_{ht}$; dark red in Fig. 4.1,
- $\{(a_i, b_1), i = \lceil \frac{n}{2} \rceil, \ldots, n\}_{ht}$; red in Fig. 4.1,
- $\{(a_{\lfloor \frac{n}{2} \rfloor}, b_j), j = 2, \ldots, \lfloor \frac{n}{2} \rfloor\}_{hh}$; gray in Fig. 4.1,
- $\{(a_i, b_2), i = \lceil \frac{n}{2} \rceil, \ldots, n\}_{hh}$; blue in Fig. 4.1,
- $\{(a_{\lceil \frac{n}{2} \rceil}, b_j), j = \lceil \frac{n}{2} \rceil, \ldots, n\}_{hh}$; light blue in Fig. 4.1.

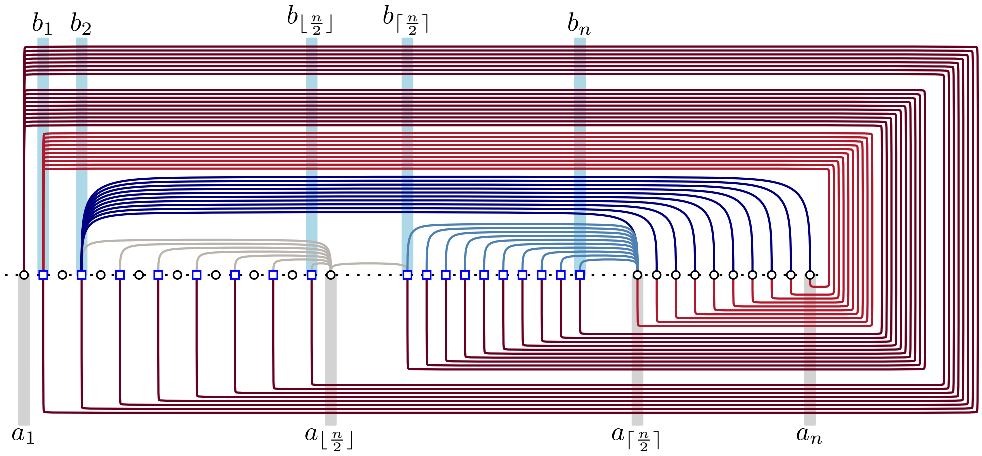

Figure 4.1: Page 1 of $\mathcal{L}$ when n is odd.

Page 2 of $\mathcal{L}$ contains the following $\frac{5n-1}{2}+1$ edges:

- $\{(a_i, b_1), i = 2, \ldots, \lfloor \frac{n}{2} \rfloor\}_{ht}$; dark red in Fig. 4.2,
- $\{(a_2, b_{\lfloor \frac{n}{2} \rfloor})\}_{ht}$; yellow in Fig. 4.2,
- $\{(a_2, b_j), j = \lceil \frac{n}{2} \rceil, \ldots, n\}_{ht}$; light red in Fig. 4.2,
- $\{(a_3, b_n)\}_{ht}$; red in Fig. 4.2,
- $\{(a_i, b_3), i = \lceil \frac{n}{2} \rceil, \ldots, n\}_{ht}$; dark blue in Fig. 4.2,
- $\{(a_{n-3}, b_j), j = \lfloor \frac{n}{2} \rfloor - 2, \ldots, \lceil \frac{n}{2} \rceil + 1\}_{hh}$; light blue in Fig. 4.2,
- $\{(a_i, b_{\lceil \frac{n}{2} \rceil + 1}), i = \lceil \frac{n}{2} \rceil + 1, \ldots, n-4\}_{hh}$; blue in Fig. 4.2,
- $\{(a_{\lceil \frac{n}{2} \rceil + 1}, b_j), j = \lceil \frac{n}{2} \rceil + 2, \ldots, n\}_{hh}$; gray in Fig. 4.2.

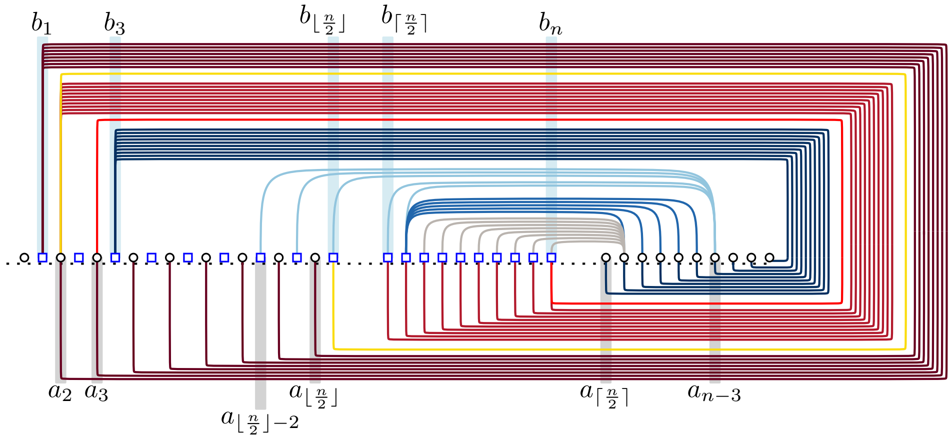

Figure 4.2: Page 2 of $\mathcal{L}$ when n is odd.

For $p = 3, 4, 5$, page p of $\mathcal{L}$ contains the following $\left(\frac{5n-1}{2}\right) + 1$ edges

- $\{(a_{p-1}, b_j), j = 2, \ldots, \lfloor \frac{n}{2} \rfloor - p + 2\}_{ht}$; dark red in Fig. 4.3,
- $\{(a_p, b_j), j = \lfloor \frac{n}{2} \rfloor - p + 2, \ldots, n - p + 2\}_{ht}$; red in Fig. 4.3,
- $\{(a_{p+1}, b_j), j = n - p + 2, \ldots, n\}_{ht}$; light red in Fig. 4.3,
- $\{(a_i, b_{p+1}), i = \lceil \frac{n}{2} \rceil, \ldots, n\}_{ht}$; dark blue in Fig. 4.3,
- $\{(a_{n+(p-5)}, b_j), j = \lfloor \frac{n}{2} \rfloor - 2, \ldots, \lceil \frac{n}{2} \rceil + (p-1)\}_{hh}$; gray in Fig. 4.3,
- $\{(a_i, b_{\lceil \frac{n}{2} \rceil + (p-1)}), i = \lceil \frac{n}{2} \rceil + (p-1), \ldots, n + (p-6)\}_{hh}$; blue in Fig. 4.3,
- $\{(a_{\lceil \frac{n}{2} \rceil + (p-1)}, b_j), j = \lceil \frac{n}{2} \rceil + p, \ldots, n\}_{hh}$; light blue in Fig. 4.3.

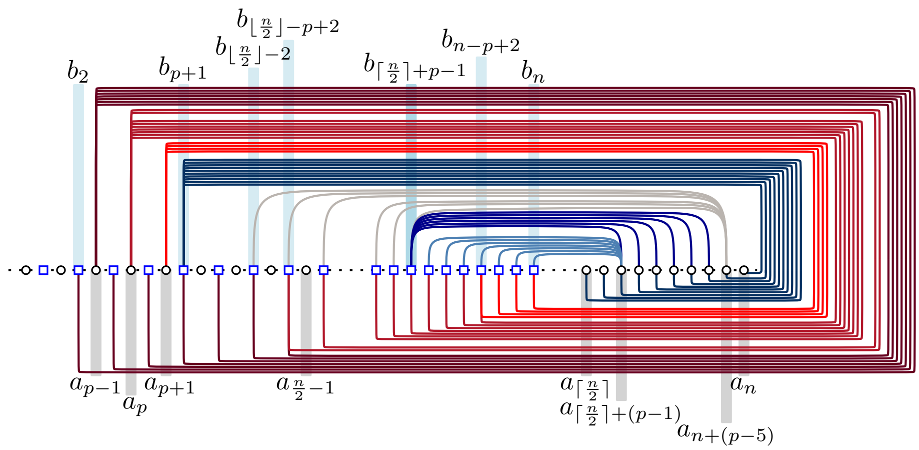

Figure 4.3: Page $p = 3, 4, 5$ of $\mathcal{L}$ when n is odd.

Page 6 of $\mathcal{L}$ contains the following $\frac{5n-1}{2} - 8$ edges:

- $\{(a_5, b_j), j = 2, \ldots, \lfloor \frac{n}{2} \rfloor - 4\}_{ht}$; dark red in Fig. 4.4,
- $\{(a_6, b_j), j = \lfloor \frac{n}{2} \rfloor - 4, \ldots, n - 4\}_{ht}$; red in Fig. 4.4,
- $\{(a_7, b_j), j = n - 4, \ldots, n\}_{ht}$; light red in Fig. 4.4,
- $\{(a_i, b_7), i = \lceil \frac{n}{2} \rceil, \ldots, n\}_{ht}$; dark blue in Fig. 4.4,
- $\{(a_i, b_{\lceil \frac{n}{2} \rceil + 5}), i = \lceil \frac{n}{2} \rceil + 5, \ldots, n)\}_{hh}$; blue in Fig. 4.4,
- $\{(a_{\lceil \frac{n}{2} \rceil + 5}, b_j), j = \lceil \frac{n}{2} \rceil + 6, \ldots, n\}_{hh}$; light red in Fig. 4.4.

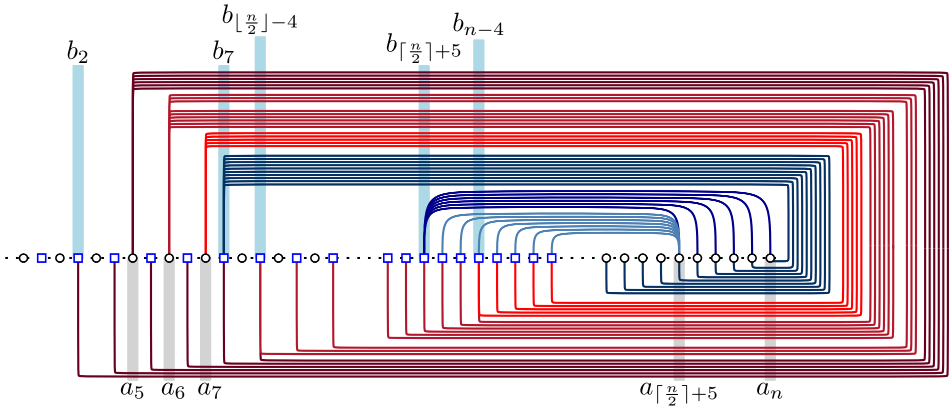

Figure 4.4: Page 6 of $\mathcal{L}$ when n is odd.

Page 7 of $\mathcal{L}$ contains the following $\frac{3n+1}{2}+4$ edges:

- $\{(a_6, b_j), j = 2, \ldots, \lfloor \frac{n}{2} \rfloor - 5\}_{ht}$; dark red in Fig. 4.5,
- $\{(a_7, b_j), j = \lfloor \frac{n}{2} \rfloor - 5, \ldots, n-5\}_{ht}$; red in Fig. 4.5,
- $\{(a_8, b_j), j = n-5, \ldots, n\}_{ht}$; light red in Fig. 4.5,
- $\{(a_i, b_8), i = \lceil \frac{n}{2} \rceil, \ldots, n\}_{ht}$; blue in Fig. 4.5,
- $\{(a_{\lfloor \frac{n}{2} \rfloor}, b_j), j = \lceil \frac{n}{2} \rceil, \ldots, \lceil \frac{n}{2} \rceil + 2)\}_{hh}$; light blue in Fig. 4.5.

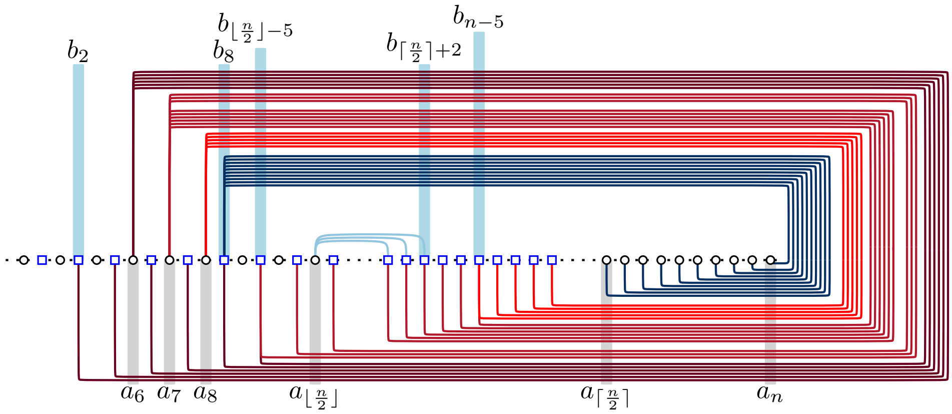

Figure 4.5: Page 7 of $\mathcal{L}$ when n is odd.

For $p = 8, \ldots, \frac{n-1}{2} - 6$, page p of $\mathcal{L}$ contains the following $\frac{5n+3}{2} - 2p + 4$ edges:

- $\{(a_{p-1}, b_j), j = 2, \ldots, \lfloor \frac{n}{2} \rfloor - p + 2\}_{ht}$; dark red in Fig. 4.6,
- $\{(a_p, b_j), j = \lfloor \frac{n}{2} \rfloor - p + 2, \ldots, n - p + 2\}_{ht}$; red in Fig. 4.6,
- $\{(a_{p+1}, b_j), j = n - p + 2, \ldots, n\}_{ht}$; light red in Fig. 4.6,
- $\{(a_i, b_{p+1}), i = \lceil \frac{n}{2} \rceil, \ldots, n\}_{ht}$; dark blue in Fig. 4.6,
- $\{(a_i, b_{\lceil \frac{n}{2} \rceil + p - 2}), i = \lceil \frac{n}{2} \rceil + p - 2, \ldots, n)\}_{hh}$; blue in Fig. 4.6,
- $\{(a_{\lceil \frac{n}{2} \rceil + p - 2}, b_j), j = \lceil \frac{n}{2} \rceil + p - 1, \ldots, n\}_{hh}$; light blue in Fig. 4.6.

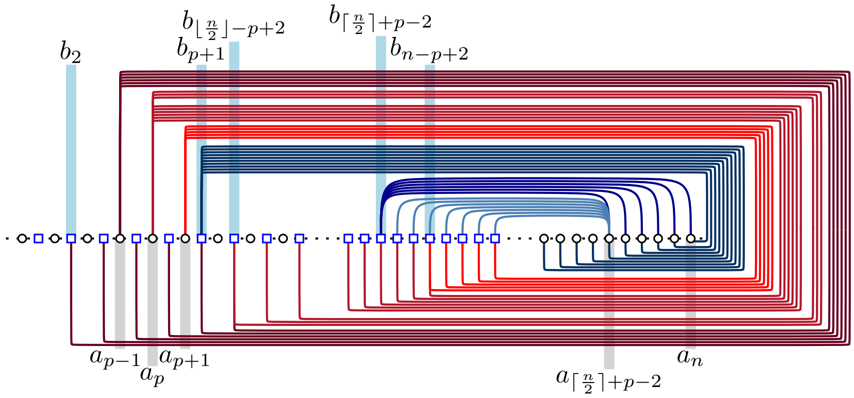

Figure 4.6: Page $p = 8, \ldots, \frac{n-1}{2} - 6$ of $\mathcal{L}$ when n is odd.

Page $\frac{n-1}{2} - 5$ of $\mathcal{L}$ contains the following 2n-3 edges:

- $\{(a_{\lfloor \frac{n}{2} \rfloor -6}, b_j), j = 2, \ldots, \lfloor \frac{n}{2} \rfloor - 7\}_{ht}$; dark red in Fig. 4.7,
- $\{(a_{(\lfloor \frac{n}{2} \rfloor -5)}, b_j), j = \lfloor \frac{n}{2} \rfloor - 7, \ldots, n - 7\}_{ht}$; red in Fig. 4.7,
- $\{(a_{\lfloor \frac{n}{2} \rfloor -4}, b_j), j = n - 7, \ldots, n\}_{ht}$; light red in Fig. 4.7,
- $\{(a_i, b_{\lfloor \frac{n}{2} \rfloor -4}), i = \lceil \frac{n}{2} \rceil, \ldots, n\}_{ht}$; light blue in Fig. 4.7,
- $\{(a_i, b_{\lfloor \frac{n}{2} \rfloor -3}), i = \lceil \frac{n}{2} \rceil + 5, \ldots, n)\}_{hh}$; blue in Fig. 4.7.

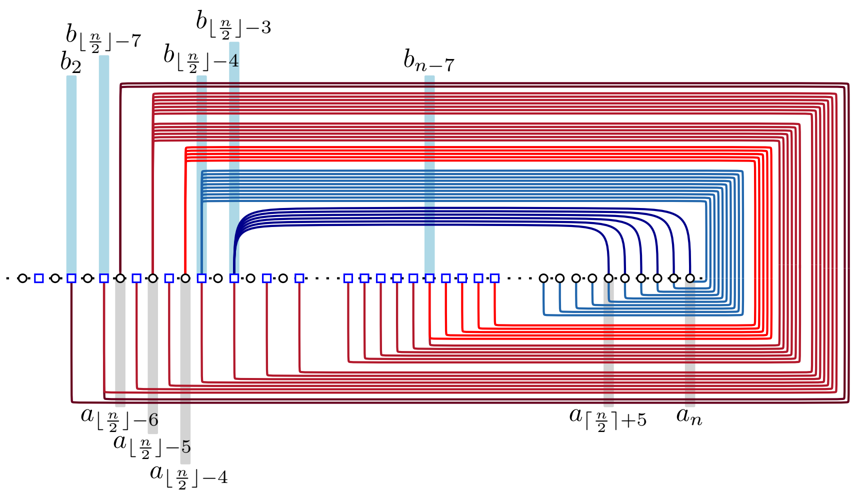

Figure 4.7: Page $\frac{n-1}{2} - 5$ of $\mathcal{L}$ when n is odd.

For $p = \frac{n-1}{2} - k$, with $k \in \{4, 3, 2\}$, page p of $\mathcal{L}$ contains the following $\frac{3n-1}{2} - 2k + 20$ edges:

- $\{(a_{p-1}, b_j), j = 2, \ldots, \lfloor \frac{n}{2} \rfloor - p - 4\}_{ht}$; dark red in Fig. 4.8,
- $\{(a_p, b_j), j = \lfloor \frac{n}{2} \rfloor - p - 4, \ldots, n - p - 4\}_{ht}$; red in Fig. 4.8,
- $\{(a_{p+1}, b_j), j = n - p - 4, \ldots, n\}_{ht}$; light red in Fig. 4.8,
- $\{(a_i, b_{p+1}), i = \lceil \frac{n}{2} \rceil, \ldots, \lceil \frac{n}{2} \rceil + k\}_{ht}$; dark pink in Fig. 4.8,
- $\{(a_i, b_{p+2}), i = \lceil \frac{n}{2} \rceil + k, \ldots, n - 8 + k\}_{ht}$; light pink in Fig. 4.8,
- $\{(a_{n-8+k}, b_j), j = \lfloor \frac{n}{2} \rfloor - 2 + k, \ldots, \lceil \frac{n}{2} \rceil\}_{ht}$; pink in Fig. 4.8,
- $\{(a_i, b_{n+(2k-9)}), i = n + (k - 8), \ldots, n\}_{ht}$; dark blue in Fig. 4.8,
- $\{(a_i, b_{n+(2k-8)}), i = n + (k - 8), \ldots, n)\}_{hh}$; blue in Fig. 4.8,
- $\{(a_{n+(k-8)}, b_j), j = n + (2k - 7), \ldots, n)\}_{hh}$; gray in Fig. 4.8.

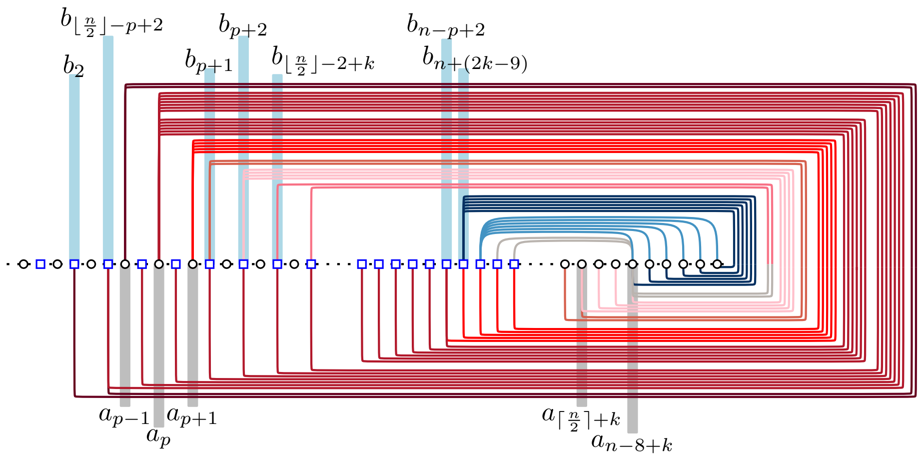

Figure 4.8: Page $p = \frac{n-1}{2} - k$, with $k \in \{4, 3, 2\}$ of $\mathcal{L}$ when n is odd.

Page $\frac{n-1}{2}-1$ of $\mathcal{L}$ contains the following $\frac{3n+1}{2}+18$ edges:

- $\{(a_{\lfloor \frac{n}{2} \rfloor -1}, b_j), j = 2, \ldots, \lceil \frac{n}{2} \rceil + 3\}_{ht}$; dark red in Fig. 4.9,
- $\{(a_{\lfloor \frac{n}{2} \rfloor}, b_j), j = \lceil \frac{n}{2} \rceil + 3, \ldots, n\}_{ht}$; red in Fig. 4.9,
- $\{(a_i, b_{\lfloor \frac{n}{2} \rfloor}), i = \lceil \frac{n}{2} \rceil, \lceil \frac{n}{2} \rceil + 1\}_{ht}$; light red in Fig. 4.9,
- $\{(a_i, b_{\lceil \frac{n}{2} \rceil}), i = \lceil \frac{n}{2} \rceil + 1, \ldots, n-7\}_{ht}$; dark pink in Fig. 4.9,
- $\{(a_i, b_{n-7}), i = \lceil \frac{n}{4} \rceil + 1, \ldots, n\}_{ht}$; pink in Fig. 4.9,
- $\{(a_i, b_{n-6}), i = \lfloor \frac{n}{4} \rfloor + 1, \ldots, n\}_{hh}$; dark blue in Fig. 4.9,
- $\{(a_{\lceil \frac{n}{4} \rceil + 1}, b_j), j = n-5, \ldots, n\}_{hh}$; blue in Fig. 4.9,
- $\{(a_{\lfloor \frac{n}{2} \rfloor -2}, b_j), j = 2, 3\}_{hh}$; gray in Fig. 4.9.

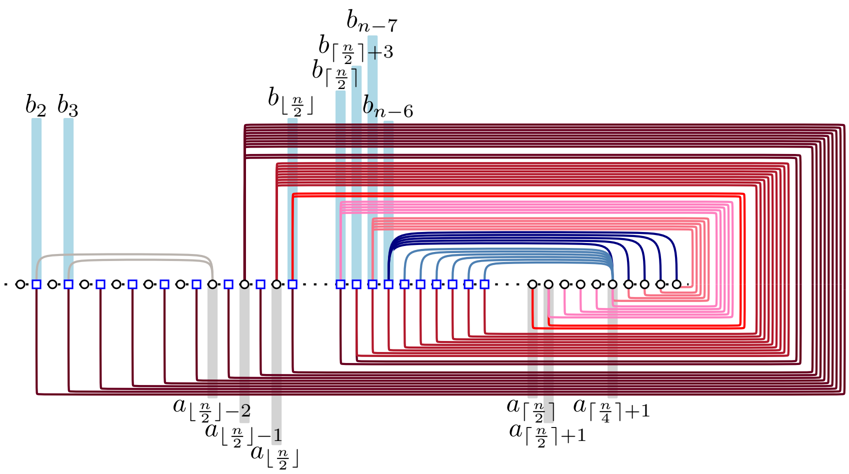

Figure 4.9: Page $\frac{n-1}{2}-1$ of $\mathcal{L}$ when n is odd.

So, in total $\mathcal{L}$ has $3n + \frac{5n-1}{2} + 1 + 3\left(\frac{5n-1}{2}+1\right) + \frac{5n-1}{2} - 8 + \frac{3n+1}{2} + 4 + \sum_{p=8}^{\frac{n-1}{2}-6} \left(\frac{5n+3}{2} - 2p + 4\right) + 2n - 3 + \sum_{k=2}^{4}(\frac{3n-1}{2} - 2k + 20) + (\frac{3n+1}{2} + 18) = n^2$ edges. Since no two edges in the same rique deviate from the properties of cylindric layouts, it follows that the rique number of $k_{n,n}$ is at most $\lfloor \frac{n-1}{2} \rfloor - 1$ when n is odd.

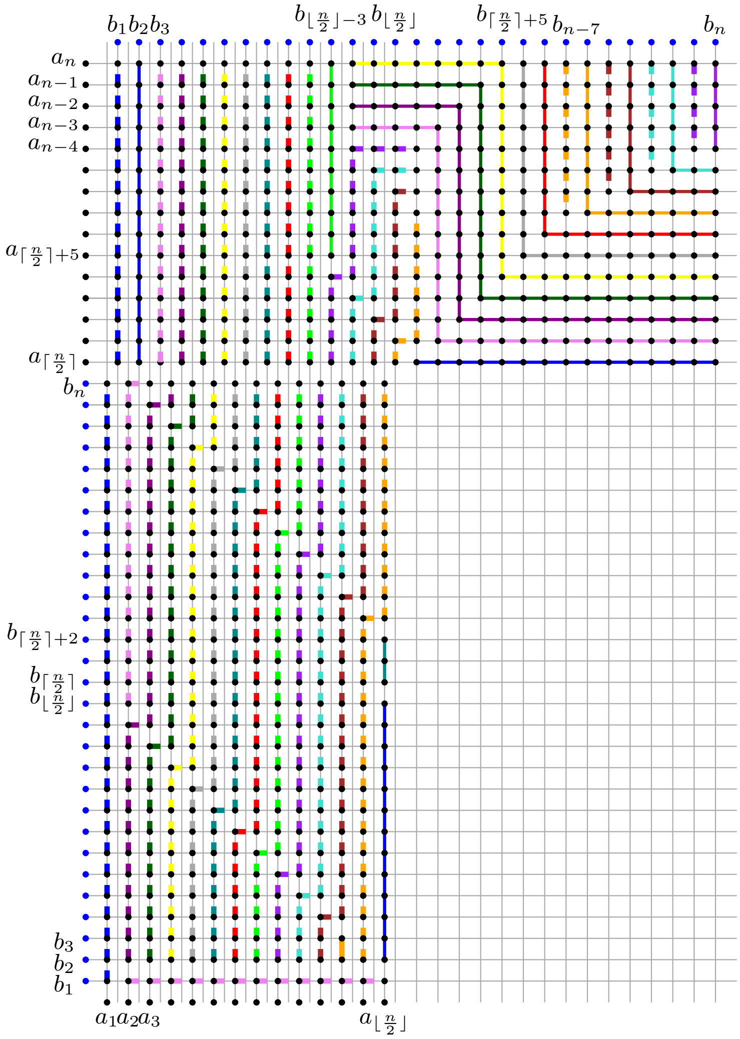

Figure 4.10: Illustration of the grid representation of a rique layout of $K_{n,n}$ when n is odd in which paths of the same color correspond to the same rique. The points of the grid that are covered by a solid (dashed) path are head-head (head-tail, respectively). Here, the "special" pages are the first (blue), second (violet), third (dark-purple), fourth (dark-green), fifth (yellow), sixth (dark-gray), eighth (cyan), $\frac{n-1}{2} - 5$ (green), $\frac{n-1}{2} - 4$ (purple), $\frac{n-1}{2} - 3$ (turquoise), $\frac{n-1}{2} - 2$ (brown), and $\frac{n-1}{2} - 1$ (orange) when n is odd. When n is even, the "special" pages are the first (blue), second (violet), third (dark-purple), fourth (dark-green), fifth (yellow), sixth (dark-gray), eighth (cyan), $\frac{n}{2} - 6$ (green), $\frac{n}{2} - 5$ (purple), $\frac{n}{2} - 4$ (turquoise), $\frac{n}{2} - 3$ (brown), and $\frac{n}{2} - 2$ (orange).

In the following, we discuss the case in which n is even and we prove that $K_{n,n}$ admits a rique layout $\mathcal{L}$ with $\frac{n}{2}-2$ riques. Let $A=\{a_1,\ldots,a_n\}$ and $B=\{b_1,\ldots,b_n\}$ be the two parts of $K_{n,n}$, such that $a_1 \prec b_1 \prec a_2 \prec b_2 \prec \cdots \prec a_{\frac{n}{2}-1} \prec b_{\frac{n}{2}-1} \prec b_{\frac{n}{2}} \prec \cdots \prec b_n \prec a_{\frac{n}{2}} \prec \cdots \prec a_n$ holds in $\mathcal{L}$. In $\mathcal{L}$, there exist 12 special riques, in particular, the ones in $\{1,2,3,4,5,6,7,\frac{n}{2}-6,\frac{n}{2}-5,\frac{n}{2}-4,\frac{n}{2}-3,\frac{n}{2}-2\}$; see Fig. 4.20.

Page 1 of $\mathcal{L}$ contains the following $3n+1$ edges:

- $\{(a_1,b_j), j=1,\ldots,n\}_{ht}$; dark red in Fig. 4.11,
- $\{(a_i,b_1), i=\frac{n}{2},\ldots,n\}_{ht}$; red in Fig. 4.11,
- $\{(a_{\frac{n}{2}-1},b_j), j=2,\ldots,\frac{n}{2}-1\}_{hh}$; light blue in Fig. 4.11,
- $\{(a_i,b_2), i=\frac{n}{2},\ldots,n\}_{hh}$; light red in Fig. 4.11,
- $\{(a_{\frac{n}{2}},b_j), j=\frac{n}{2},\ldots,n\}_{hh}$; blue in Fig. 4.11.

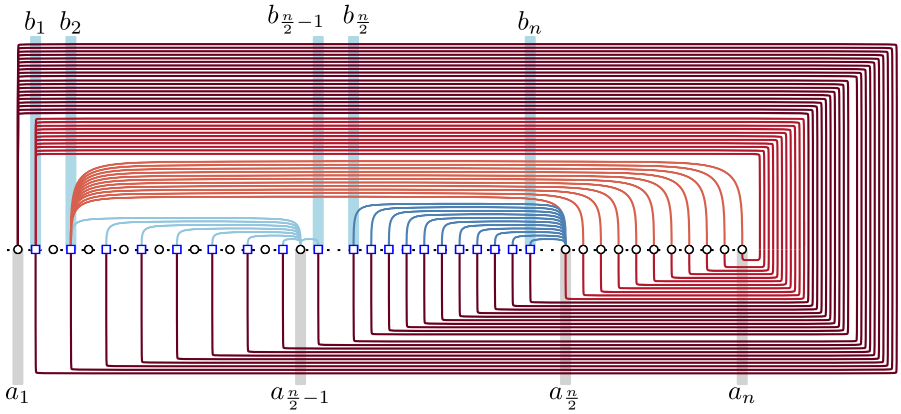

Figure 4.11: Page 1 of $\mathcal{L}$ when n is even.

Page 2 of $\mathcal{L}$ contains the following $\frac{5n}{2} + 2$ edges:

- $\{(a_i, b_1), i = 2, \ldots, \frac{n}{2} - 1\}_{ht}$; dark red in Fig. 4.12,
- $\{(a_2, b_{\frac{n}{2}-1})\}_{ht}$; orange in Fig. 4.12,
- $\{(a_2, b_j), j = \frac{n}{2}, \ldots, n\}_{ht}$; red in Fig. 4.12,
- $\{(a_3, b_n)\}_{ht}$; light red in Fig. 4.12,
- $\{(a_i, b_3), i = \frac{n}{2}, \ldots, n\}_{ht}$;light blue in Fig. 4.12,
- $\{(a_{n-3}, b_j), j = \frac{n}{2} - 3, \ldots, \frac{n}{2} + 1\}_{hh}$; blue in Fig. 4.12,
- $\{(a_i, b_{\frac{n}{2}+1}), i = \frac{n}{2} + 1, \ldots, n - 4\}_{hh}$; dark blue in Fig. 4.12,
- $\{(a_{\frac{n}{2}+1}, b_j), j = \frac{n}{2} + 2, \ldots, n\}_{hh}$; gray in Fig. 4.12.

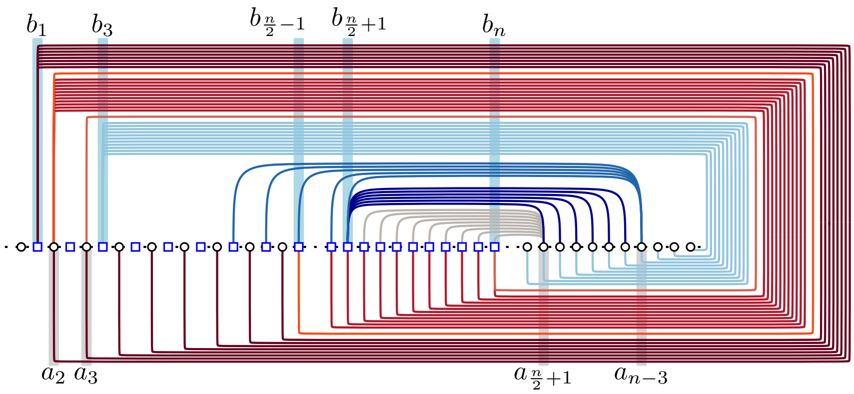

Figure 4.12: Page 2 of $\mathcal{L}$ when n is even.

For $p = 3, 4, 5$, page p of $\mathcal{L}$ contains the following $\frac{5n}{2} + 2$ edges

- $\{(a_{p-1}, b_j), j = 2, \ldots, \frac{n}{2} - p + 1\}_{ht}$; dark red in Fig. 4.13,
- $\{(a_p, b_j), j = \frac{n}{2} - p + 1, \ldots, n - p + 2\}_{ht}$; red in Fig. 4.13,
- $\{(a_{p+1}, b_j), j = n - p + 2, \ldots, n\}_{ht}$; light red in Fig. 4.13,
- $\{(a_i, b_{p+1}), i = \frac{n}{2}, \ldots, n\}_{ht}$; dark blue in Fig. 4.13,
- $\{(a_{n+p-6}, b_j), j = \frac{n}{2} - 3, \ldots, \frac{n}{2} + p - 1\}_{hh}$; light blue in Fig. 4.13,
- $\{(a_i, b_{\frac{n}{2}+(p-1)}), i = \frac{n}{2} + (p-1), \ldots, n + (p-6)\}_{hh}$; blue in Fig. 4.13,
- $\{(a_{\frac{n}{2}+(p-1)}, b_j), j = \frac{n}{2} + p, \ldots, n\}_{hh}$; gray in Fig. 4.13.

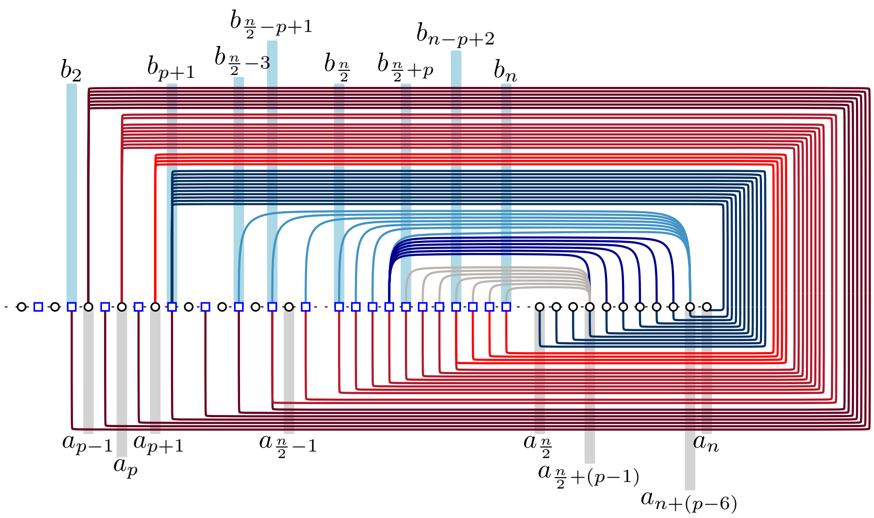

Figure 4.13: Page $p = 3, 4, 5$ of $\mathcal{L}$ when n is even.

Page 6 of $\mathcal{L}$ contains the following $\frac{5n}{2} - 7$ edges:

- $\{(a_5, b_j), j = 2, \ldots, \frac{n}{2} - 5\}_{ht}$; dark red in Fig. 4.14,
- $\{(a_6, b_j), j = \frac{n}{2} - 5, \ldots, n - 4\}_{ht}$; red in Fig. 4.14,
- $\{(a_7, b_j), j = n - 4, \ldots, n\}_{ht}$; light red in Fig. 4.14,
- $\{(a_i, b_7), i = \frac{n}{2}, \ldots, n\}_{ht}$; dark blue in Fig. 4.14,
- $\{(a_i, b_{\frac{n}{2}+5}), i = \frac{n}{2} + 5, \ldots, n)\}_{hh}$; blue in Fig. 4.14,
- $\{(a_{\frac{n}{2}+5}, b_j), j = \frac{n}{2} + 6, \ldots, n\}_{hh}$; gray in Fig. 4.14.

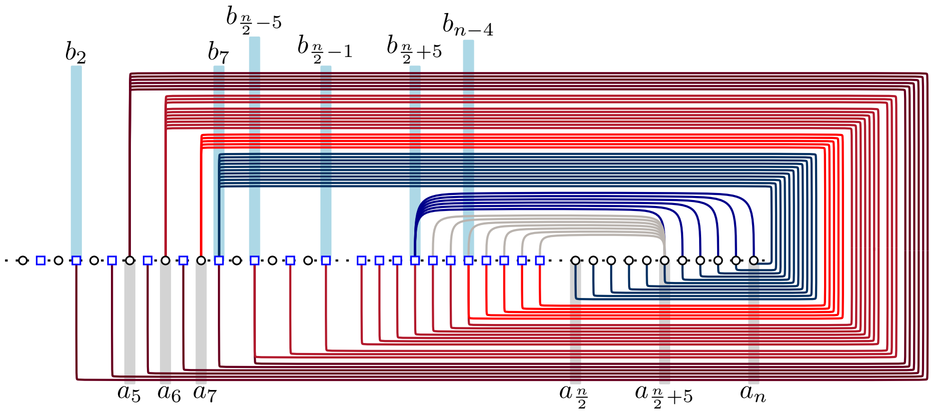

Figure 4.14: Page 6 of $\mathcal{L}$ when n is even.

Page 7 of $\mathcal{L}$ contains the following $\frac{3n}{2} + 23$ edges:

- $\{(a_6, b_j), j = 2, \ldots, \frac{n}{2} - 6\}_{ht}$; dark red in Fig. 4.15,
- $\{(a_7, b_j), j = \frac{n}{2} - 6, \ldots, n - 5\}_{ht}$; red in Fig. 4.15,
- $\{(a_8, b_j), j = n - 5, \ldots, n\}_{ht}$; light red in Fig. 4.15,
- $\{(a_i, b_8), i = \frac{n}{2}, \ldots, n\}_{ht}$; dark blue in Fig. 4.15,
- $\{(a_{\frac{n}{2}-1}, b_j), j = \frac{n}{2}, \ldots, \frac{n}{2} + 3)\}_{hh}$; gray in Fig. 4.15,
- $\{(a_{n-8}, b_j), j = n - 8, \ldots, n\}_{hh}$; blue in Fig. 4.15,
- $\{(a_i, b_{n-8}), i = n - 7, \ldots, n\}_{hh}$; light blue in Fig. 4.15.

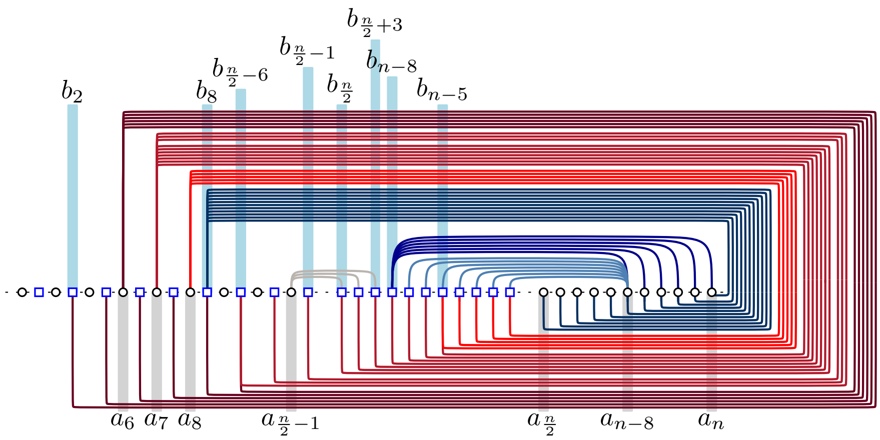

Figure 4.15: Page 7 of $\mathcal{L}$ when n is even.

For $p = 8, \ldots, \frac{n}{2} - 7$, page p of $\mathcal{L}$ contains the following $\frac{5n}{2} - 2p + 7$ edges:

- $\{(a_{p-1}, b_j), j = 2, \ldots, \frac{n}{2} - p + 1\}_{ht}$; dark red in Fig. 4.16,
- $\{(a_p, b_j), j = \frac{n}{2} - p + 1, \ldots, n - p + 2\}_{ht}$; red in Fig. 4.16,
- $\{(a_{p+1}, b_j), j = n - p + 2, \ldots, n\}_{ht}$; light red in Fig. 4.16,
- $\{(a_i, b_{p+1}), i = \frac{n}{2}, \ldots, n\}_{ht}$; dark blue in Fig. 4.16,
- $\{(a_i, b_{\frac{n}{2}+p-2}), i = \frac{n}{2} + (p-2), \ldots, n)\}_{hh}$; blue in Fig. 4.16,
- $\{(a_{\frac{n}{2}+(p-2)}, b_j), j = \frac{n}{2} + (p-1), \ldots, n\}_{hh}$; light blue in Fig. 4.16.

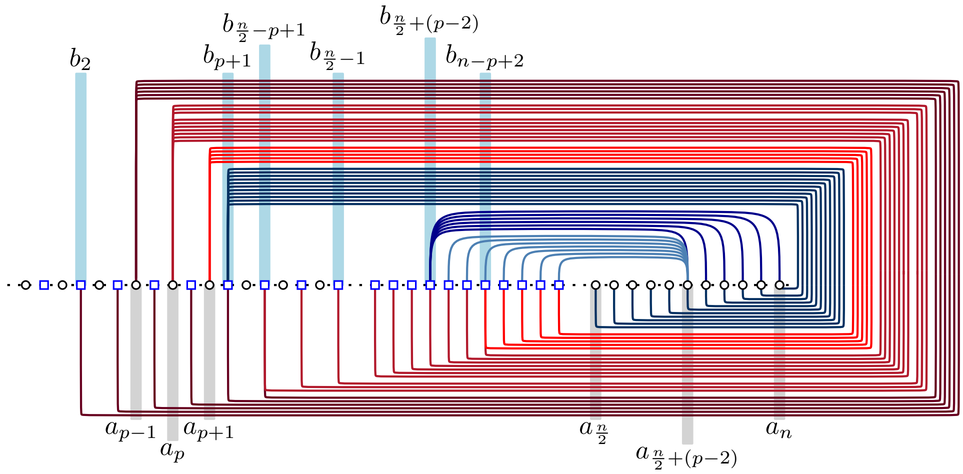

Figure 4.16: Page $p = 8, \ldots, \frac{n}{2} - 7$ of $\mathcal{L}$ when n is even.

Page $\frac{n}{2} - 6$ of $\mathcal{L}$ contains the following 2n-2 edges:

- $\{(a_{\frac{n}{2}-7}, b_j), j = 2, \ldots, \frac{n}{2} - 8\}_{ht}$; dark red in Fig. 4.17,
- $\{(a_{\frac{n}{2}-6}, b_j), j = \frac{n}{2} - 8, \ldots, n - 7\}_{ht}$; red in Fig. 4.17,
- $\{(a_{\frac{n}{2}-5}, b_j), j = n - 7, \ldots, n\}_{ht}$; light red in Fig. 4.17,
- $\{(a_i, b_{\frac{n}{2}-5}), i = \frac{n}{2}, \ldots, n\}_{ht}$; blue in Fig. 4.17,
- $\{(a_i, b_{\frac{n}{2}-4}), i = \frac{n}{2} + 5, \ldots, n)\}_{hh}$; dark blue in Fig. 4.17.

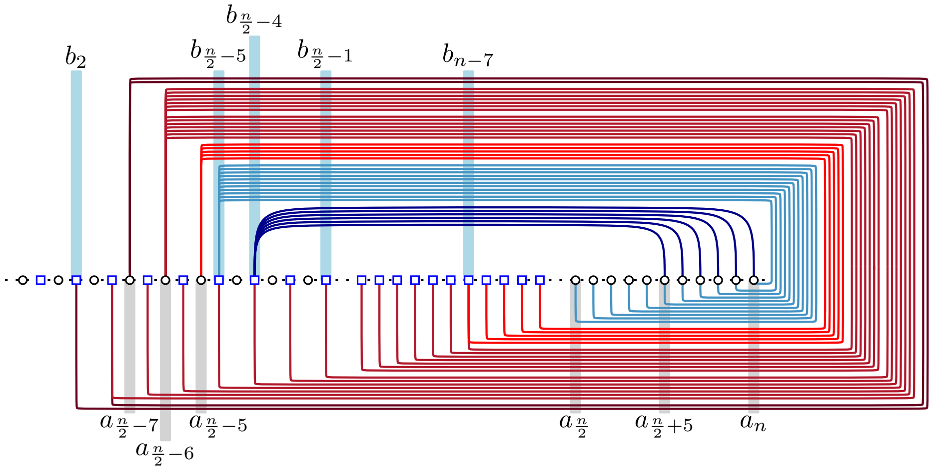

Figure 4.17: Page $\frac{n}{2} - 6$ of $\mathcal{L}$ when n is even.

For $p = \frac{n}{2} - k$, with $k \in \{5, 4, 3\}$, page p of $\mathcal{L}$ contains the following $\frac{3n}{2} - 2k + 22$ edges:

- $\{(a_{p-1}, b_j), j = 2, \ldots, \frac{n}{2} - p + 1)\}_{ht}$; dark red in Fig. 4.18,
- $\{(a_p, b_j), j = \frac{n}{2} - p + 1, \ldots, n - p + 2)\}_{ht}$; red in Fig. 4.18,
- $\{(a_{p+1}, b_j), j = n - p + 2, \ldots, n\}_{ht}$; light red in Fig. 4.18,
- $\{(a_i, b_{p+1}), i = \frac{n}{2}, \ldots, \frac{n}{2} + (k-1)\}_{ht}$; pink in Fig. 4.18,
- $\{(a_i, b_{p+2}), i = \frac{n}{2} + (k-1), \ldots, n - 8 + k\}_{ht}$; light pink in Fig. 4.18,
- $\{(a_{n-8+k}, b_j), j = \frac{n}{2} - 3 - k, \ldots, \frac{n}{2}\}_{ht}$; blue in Fig. 4.18,
- $\{(a_i, b_{n+(2k-11)}), i = n - 8 + k, \ldots, n\}_{ht}$; light blue in Fig. 4.18,
- $\{(a_i, b_{n+(2k-10)}), i = n - 8 + k, \ldots, n\}_{hh}$; dark blue in Fig. 4.18,
- $\{(a_{n-8+k}, b_j), j = n + (2k-9), \ldots, n\}_{hh}$; gray in Fig. 4.18.

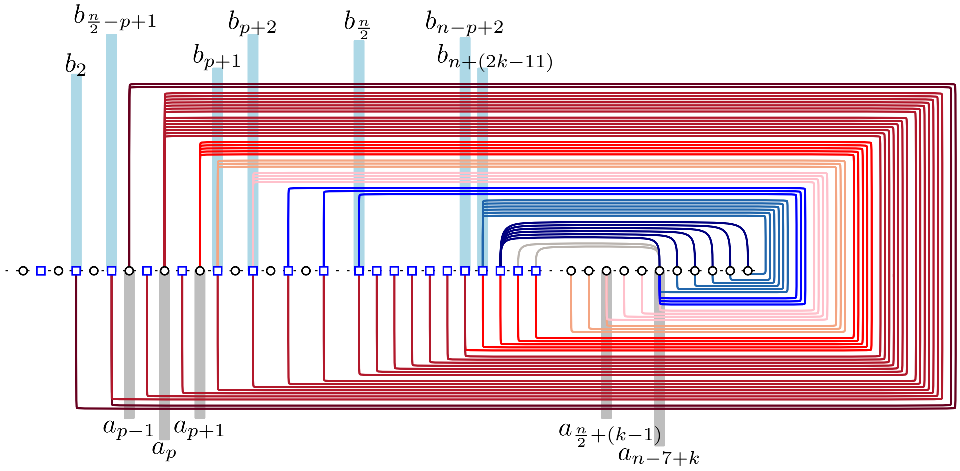

Figure 4.18: Page $p = \frac{n}{2} - k$, with $k \in \{5, 4, 3\}$ of $\mathcal{L}$ when n is even.

Page $\frac{n}{2}-2$ of $\mathcal{L}$ contains the following $\frac{3n}{2}+19$ edges:

- $\{(a_{\frac{n}{2}-2}, b_j), j = 2, \ldots, \frac{n}{2}+4\}_{ht}$; dark red in Fig. 4.19,
- $\{(a_{\frac{n}{2}-1}, b_j), j = \frac{n}{2}+4, \ldots, n\}_{ht}$; red in Fig. 4.19,
- $\{(a_i, b_{\frac{n}{2}-1}), i = \frac{n}{2}, \frac{n}{2}+1\}_{ht}$; light red in Fig. 4.19,
- $\{(a_i, b_{\frac{n}{2}}), i = \frac{n}{2}+1, \ldots, n-7\}_{ht}$; pink in Fig. 4.19,
- $\{(a_i, b_{n-7}), i = \frac{n}{4}+1, \ldots, n\}_{ht}$; dark blue in Fig. 4.19,
- $\{(a_i, b_{n-6}), i = \frac{n}{4}+1, \ldots, n\}_{hh}$; light blue in Fig. 4.19,
- $\{(a_{\frac{n}{4}+1}, b_j), j = n-5, \ldots, n\}_{hh}$; gray in Fig. 4.19,
- $\{(a_{\frac{n}{2}-3}, b_j), j = 2, 3\}_{hh}$; blue in Fig. 4.19.

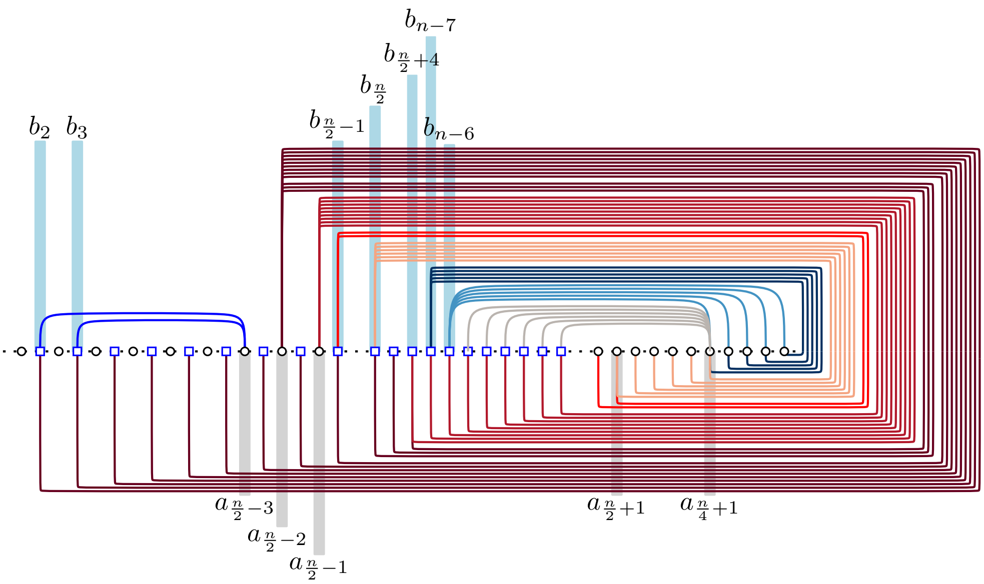

Figure 4.19: Page $p = \frac{n}{2}-2$ of $\mathcal{L}$ when n is even.

So, in total $\mathcal{L}$ has n^2 edges. Since no two edges in the same rique deviate from the properties of cylindric layouts, it follows that the rique number of $K_{n,n}$ is at most $\frac{n}{2}-2$ when n is even.

□

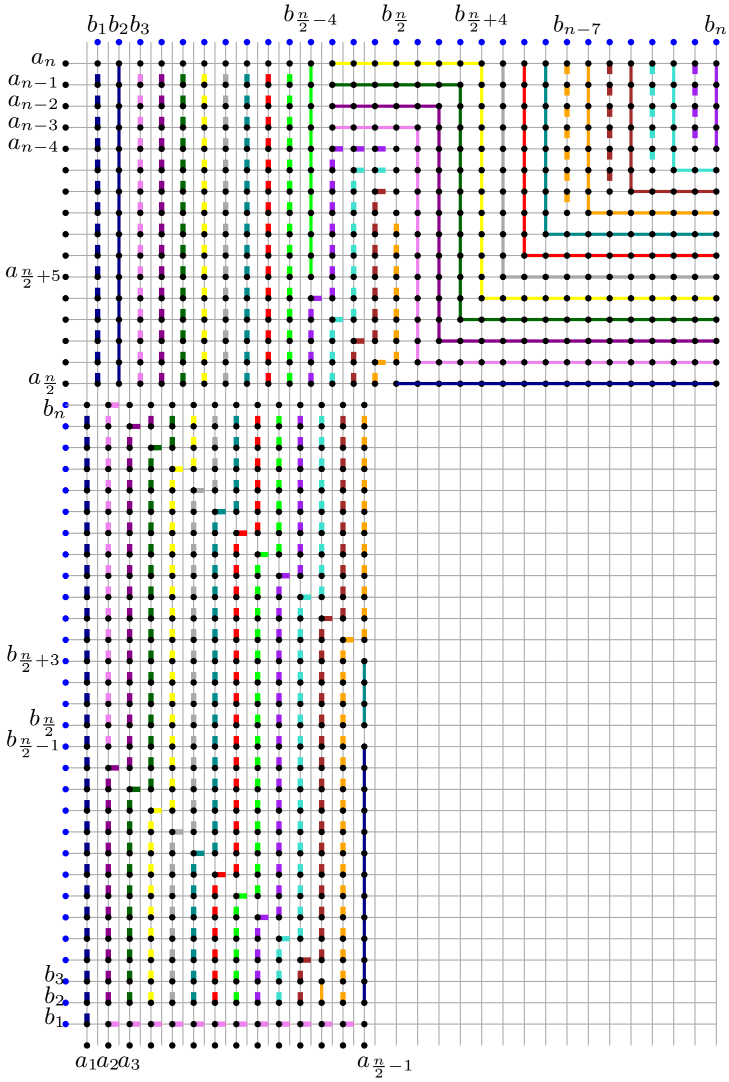

Figure 4.20: Illustration of the grid representation of a rique layout of $K_{n,n}$ when n is even, in which paths of the same color correspond to the same rique. The points of the grid that are covered by a solid (dashed) path are head-head (head-tail, respectively). Here, the "special" pages are the first (blue), second (violet), third (dark-purple), fourth (dark-green), fifth (yellow), sixth (dark-gray), eighth (cyan), $\frac{n-1}{2} - 5$ (green), $\frac{n-1}{2} - 4$ (purple), $\frac{n-1}{2} - 3$ (turquoise), $\frac{n-1}{2} - 2$ (brown), and $\frac{n-1}{2} - 1$ (orange) when n is odd. When n is even, the "special" pages are the first (blue), second (violet), third (dark-purple), fourth (dark-green), fifth (yellow), sixth (dark-gray), eighth (cyan), $\frac{n}{2} - 6$ (green), $\frac{n}{2} - 5$ (purple), $\frac{n}{2} - 4$ (turquoise), $\frac{n}{2} - 3$ (brown), and $\frac{n}{2} - 2$ (orange).

CHAPTER 5

SAT Formulation and Named Graphs

As part of this thesis, we implemented both SAT-based approaches for testing whether a given graph admits a rique layout in a certain number of riques described in Chapter 2. Our implementation has been incorporated in [6] and the corresponding source code has become available at `https://github.com/linear-layouts/SAT`. Note that even though Rieger's approach [30] is tailored for deque layouts, it is not difficult to be adjusted to rique layouts. Recall that for each edge e and each x in $\{hh, ht, th, tt\}$ in her approach there exists a variable $\tau_p(e, x)$ with the following meaning.

$\tau_p(e, x)$ is `true`, if and only if the type of edge e at page p is x.

We adjusted her approach for the case where p is a rique, by introducing for each edge e the following clause forbidding tail-head and tail-tail edges:

$$\neg\tau_p(e, th) \wedge \neg\tau_p(e, tt)$$

We used our implementation to compute the rique number of different graphs that are named in the literature. Our source was the following wikipedia page:

`https://en.wikipedia.org/wiki/List_of_graphs`

In this wikipedia page the graphs are grouped into the following categories. We present our findings on their rique numbers using this grouping (we omitted groups containing very large graphs since these could not be tested).

- Individual graphs; see Section 5.1
- Strongly regular graphs; see Section 5.2
- Symmetric graphs; see Section 5.3
- Semi-symmetric graphs; see Section 5.4
- Fullerene graphs; see Section 5.5
- Platonic solids; see Section 5.6
- Truncated solids; see Section 5.7
- Snarks; see Section 5.8

5.1 Individual graphs

Table 5.1: The rique number of individual graphs

Graph	$\|V\|$	$\|E\|$	$rn(G)$	Graph	$\|V\|$	$\|E\|$	$rn(G)$
Ellingham–Horton 54	54	81	2	Meredith	70	140	2
Ellingham–Horton 78	78	117	2	Hoffman	16	32	2
Windmill Wd(5,4)	17	40	2	Herschel	11	18	1
Balaban 10-cage	70	105	2	Franklin	12	18	2
Balaban 11-cage	112	168	2	Chvátal	12	24	2
Tutte's fragment	18	24	1	Golomb	10	18	1
Goldner–Harary	11	27	2	Poussin	15	39	1
Wiener–Araya	42	67	1	Wagner	8	12	2
Harries–Wong	70	105	2	Horton	96	144	2
Moser spindle	7	11	1	McGee	24	36	2
Bidiakis cube	12	18	1	Harries	70	105	2
Brinkmann	21	42	2	Frucht	12	18	1
Markström	24	36	1	Kittell	23	63	1
Robertson	19	38	2	Errera	17	45	1
Sousselier	16	27	2	Dürer	12	18	1
Butterfly	5	6	1	Tutte	46	69	1
Diamond	4	5	1	Wells	32	80	3
Sylvester	36	90	3	Holt	27	54	2
Grötzsch	11	20	2	Bull	5	5	1

5.2 Strongly Regular Graphs

Table 5.2: The rique number of strongly regular graphs

Graph	$\|V\|$	$\|E\|$	$rn(G)$
Shrikhande	16	48	2
Petersen	10	15	2
Clebsch	16	40	2
Paley	13	39	2

5.3 Symmetric graphs

Table 5.3: The rique number of symmetric graphs

Graph	$\|V\|$	$\|E\|$	rn
Möbius–Kantor	16	24	2
Tutte–Coxeter	30	45	2
Biggs–Smith	102	153	3
Desargues	20	30	2
Heawood	14	21	2
Coxeter	28	42	2
Pappus	18	27	2
Foster	90	135	3
Nauru	24	36	2
Klein	56	84	2
Dyck	32	48	2

5.4 Semi-symmetric graphs

Table 5.4: The rique number of semi-symmetric graphs

Graph	$\|V\|$	$\|E\|$	$rn(G)$
Tutte 12-cage	126	189	3
Ljubljana	112	168	3
Folkman	20	40	2
Gray	54	81	2

5.5 Fullerene graphs

Table 5.5: The rique number of Fullerene graphs

Graph	$\|V\|$	$\|E\|$	$rn(G)$
Hexagonal Truncated Trapezohedron	24	36	1
Truncated Tcosahedral	60	90	1
Dodecahedral	20	30	1
70-fullerene	70	105	1
26-fullerene	26	39	1

5.6 Platonic solids graphs

Table 5.6: The rique number of platonic solids graphs

Graph	$\|V\|$	$\|E\|$	rn
Dodecahedron	20	30	1
Icosahedron	12	30	1
Octahedron	6	12	1
Cube	8	12	1

5.7 Truncated solids graphs

Table 5.7: The rique number of truncated solids graphs

Graph	$\|V\|$	$\|E\|$	$rn(G)$
Truncated cube	24	36	1
Dodecahedron	60	90	1
Tetrahedron	12	18	1
Octahedron	24	36	1
Icosahedron	60	90	1

5.8 Snarks

Table 5.8: The rique number of snarks

Graph	$\|V\|$	$\|E\|$	$rn(G)$
Loupekine (first)	22	33	2
Loupekine (second)	22	33	2
Blanuša (first)	18	27	2
Blanuša (second)	18	27	2
Flower (first)	20	30	2
Flower (second)	28	42	2
Double-star	30	45	2
Szekeres	50	75	2
Watkins	50	75	2
Tietze	12	18	2

5.9 Gallery of Named Graphs

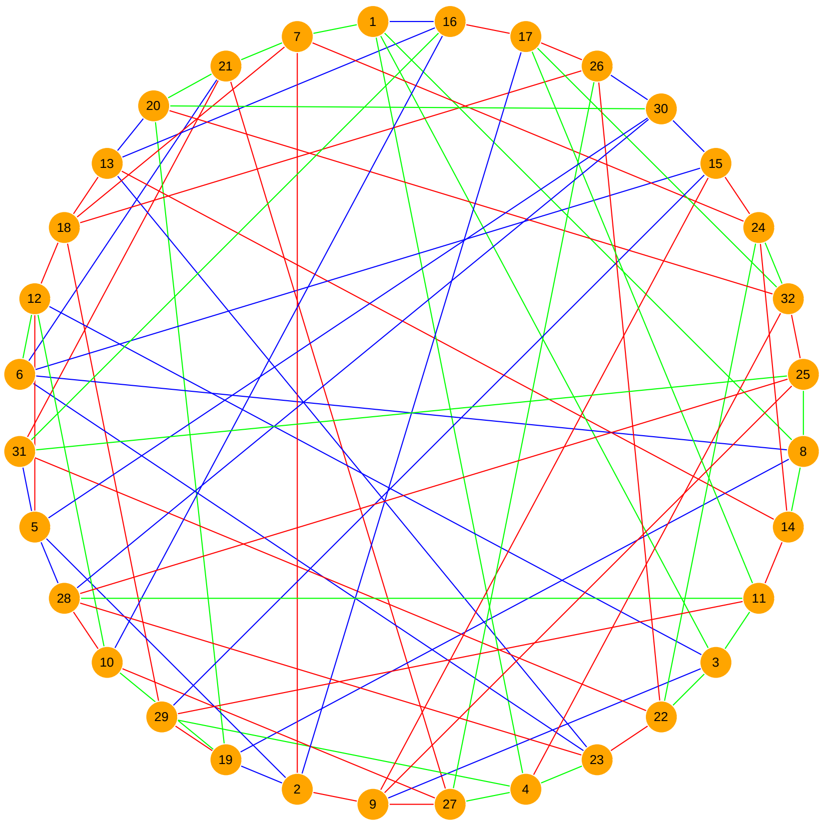

Figure 5.1: Well's graph where in the rique layout that follows the red edges form the first page, the blue edges form the second page, and the green edges form the third page.

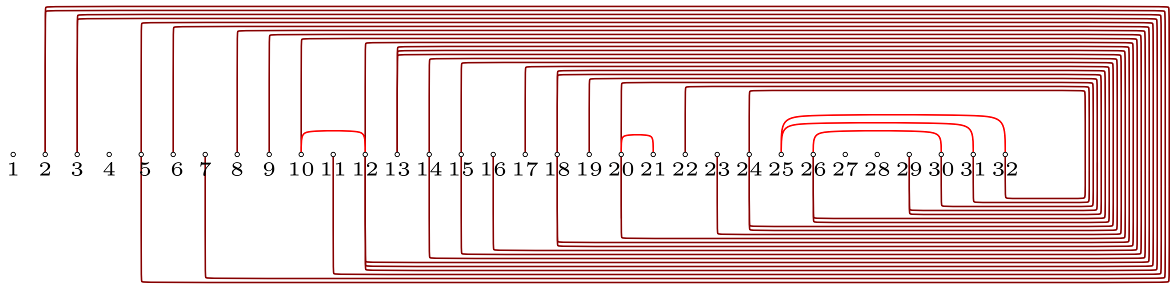

Figure 5.2: Illustration of Page 1 of Well's graph

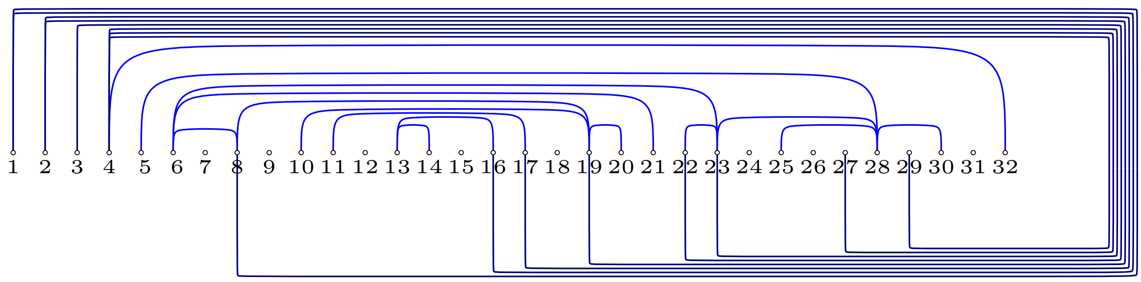

Figure 5.3: Illustration of Page 2 of Well's graph

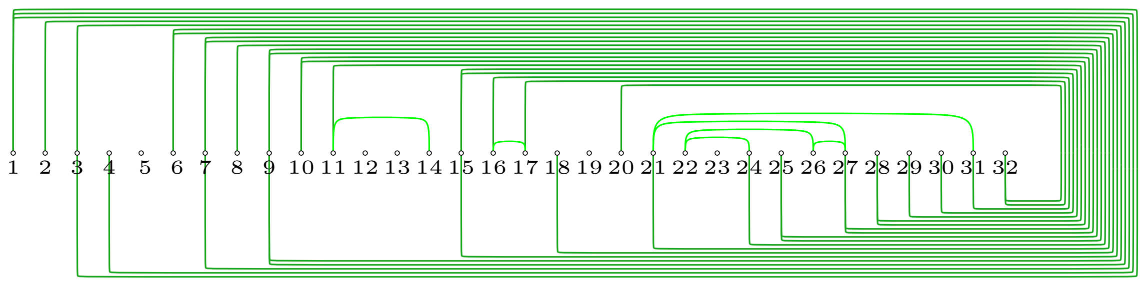

Figure 5.4: Illustration of Page 3 of Well's graph

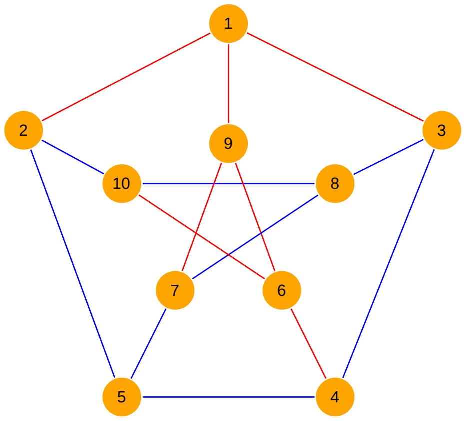

Figure 5.5: Illustration of Peterson's graph where in the rique layout that follows the red edges form the first page and the blue edges form the second page.

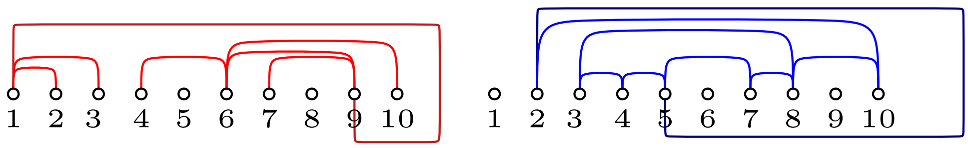

(a) (b)

Figure 5.6: Illustration of (a) Page 1 and (b) Page 2 of Peterson's graph.

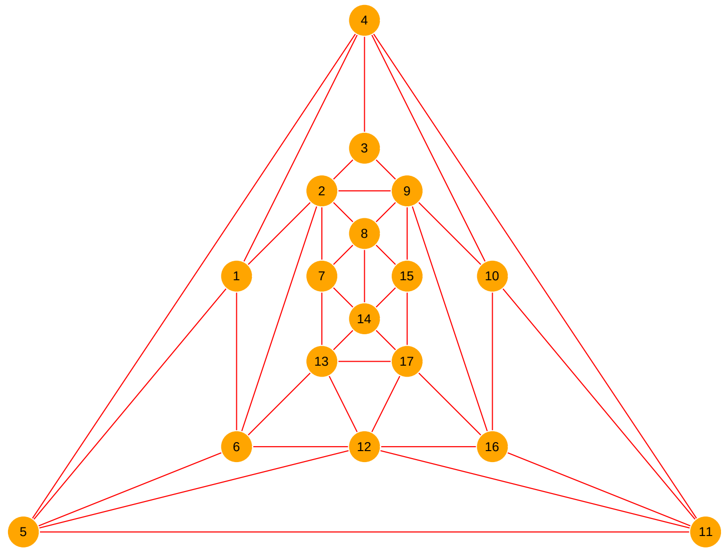

Figure 5.7: Errera's graph

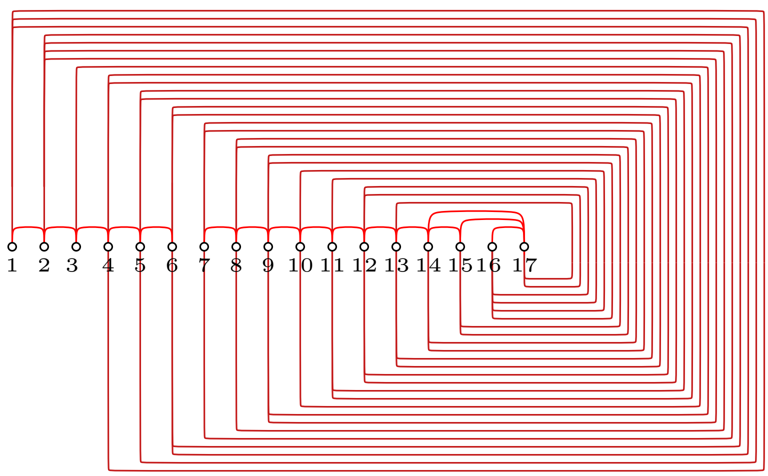

Figure 5.8: Illustration of the rique layout of Errera's graph

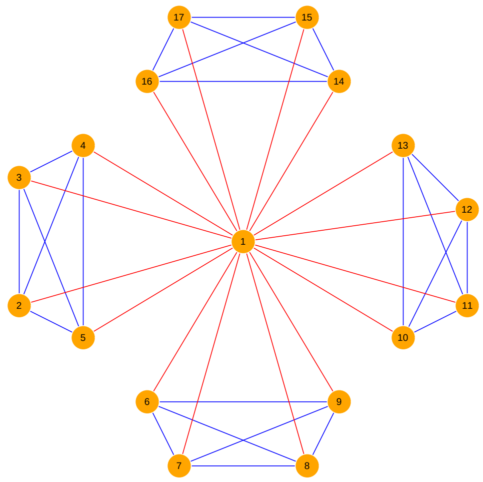

Figure 5.9: Illustration of the Windmill$(5, 4)$

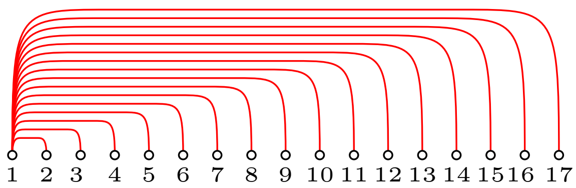

Figure 5.10: Illustration of Page 1 of Windmill

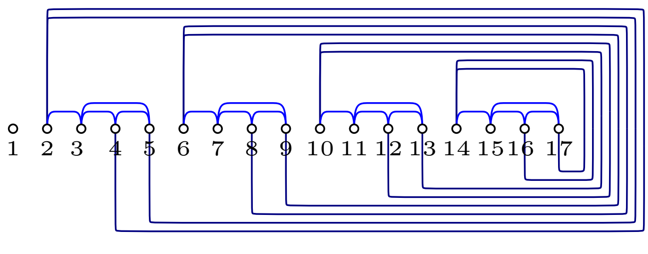

Figure 5.11: Illustration of Page 2 of Windmill

CHAPTER 6

CONCLUSIONS

In conclusion, the focus of this thesis was on rique layouts of graphs that utilize the well-known restricted-input double-ended queue data structure to determine which edges can exist in the same page. We examined complete graphs and complete bipartite graphs and we presented improved upper bounds on their rique numbers, where the later represents the minimum number of pages required for any rique layout of them. In our research, we improved the upper bound for complete graphs and introduced a new one for complete bipartite graphs of equal parts.

By employing a SAT-based approach, we demonstrated that the first bound is tight for all complete graphs with up to 30 vertices. To this end, we conjecture that our bound for complete graphs is tight. This might also hold for our bound on the rique number of complete bipartite graphs, since we have checked with our SAT implementation that the bound is tight for all complete bipartite graphs (with equal parts) up to $K_{21,21}$.

We deem important to mention that there exist several questions unanswered about the rique numbers of other graph families. As an example, we mention the class of planar graphs. For this class of graphs, we know that their rique number is at least 2 (e.g., the Golden-Harary graph is a graph requiring two riques; see Chapter 5). However, it is still unknown if there exists a planar graph with rique number of at least 3. Using our SAT formulation, we tried to find one, but without success. At the point of writing this thesis, parts ofthis thesis have been submited for publication at CCCG 2023.

Bibliography

[1] Alam, J. M., Bekos, M. A., Gronemann, M., Kaufmann, M., and Pupyrev, S. Queue layouts of planar 3-trees. *Algorithmica 82*, 9 (2020), 2564–2585.

[2] Alam, J. M., Bekos, M. A., Gronemann, M., Kaufmann, M., and Pupyrev, S. The mixed page number of graphs. *Theor. Comput. Sci. 931* (2022), 131–141.

[3] Auer, C., Bachmaier, C., Brandenburg, F., Brunner, W., and Gleissner, A. Plane drawings of queue and deque graphs. In *Graph Drawing - 18th International Symposium, GD 2010, Konstanz, Germany, September 21-24, 2010. Revised Selected Papers* (2010), U. Brandes and S. Cornelsen, Eds., vol. 6502 of *Lecture Notes in Computer Science*, Springer, pp. 68–79.

[4] Bekos, M. A., Felsner, S., Kindermann, P., Kobourov, S. G., Kratochvíl, J., and Rutter, I. The rique-number of graphs. In *Graph Drawing and Network Visualization - 30th International Symposium, GD 2022, Tokyo, Japan, September 13-16, 2022, Revised Selected Papers* (2022), P. Angelini and R. von Hanxleden, Eds., vol. 13764 of *Lecture Notes in Computer Science*, Springer, pp. 371–386.

[5] Bekos, M. A., Gronemann, M., and Raftopoulou, C. N. On the queue number of planar graphs. *CoRR abs/2106.08003* (2021).

[6] Bekos, M. A., Haug, M., Kaufmann, M., and Männecke, J. An online framework to interact and efficiently compute linear layouts of graphs. *CoRR abs/2003.09642* (2020).

[7] Bekos, M. A., Kaufmann, M., Klute, F., Pupyrev, S., Raftopoulou, C. N., and Ueckerdt, T. Four pages are indeed necessary for planar graphs. *J. Comput. Geom. 11*, 1 (2020), 332–353.

[8] Bekos, M. A., Kaufmann, M., and Zielke, C. The book embedding problem from a sat-solving perspective. In *Graph Drawing and Network Visualization - 23rd International Symposium, GD 2015, Los Angeles, CA, USA, September 24-26, 2015, Revised Selected Papers* (2015), E. D. Giacomo and A. Lubiw, Eds., vol. 9411 of *Lecture Notes in Computer Science*, Springer, pp. 125–138.

[9] Bernhart, F., and Kainen, P. C. The book thickness of a graph. *J. Comb. Theory, Ser. B 27*, 3 (1979), 320–331.

[10] Bhatt, S. N., Chung, F. R. K., Leighton, F. T., and Rosenberg, A. L. Scheduling tree-dags using FIFO queues: A control-memory trade-off. *J. Parallel Distributed Comput. 33*, 1 (1996), 55–68.

[11] Dujmovic, V., Eppstein, D., Hickingbotham, R., Morin, P., and Wood, D. R. Stack-number is not bounded by queue-number. *Comb. 42*, 2 (2022), 151–164.

[12] Dujmovic, V., Joret, G., Micek, P., Morin, P., Ueckerdt, T., and Wood, D. R. Planar graphs have bounded queue-number. *J. ACM 67*, 4 (2020), 22:1–22:38.

[13] Dujmovic, V., Morin, P., and Wood, D. R. Layout of graphs with bounded tree-width. *SIAM J. Comput. 34*, 3 (2005), 553–579.

[14] Dujmović, V., and Wood, D. R. On linear layouts of graphs. *Discrete Mathematics & Theoretical Computer Science 6*, 2 (2004), 339–358.

[15] Dujmovic, V., and Wood, D. R. Stacks, queues and tracks: Layouts of graph subdivisions. *Discret. Math. Theor. Comput. Sci. 7*, 1 (2005), 155–202.

[16] Enomoto, H., Nakamigawa, T., and Ota, K. On the pagenumber of complete bipartite graphs. *J. Comb. Theory, Ser. B 71*, 1 (1997), 111–120.

[17] Felsner, S., Merker, L., Ueckerdt, T., and Valtr, P. Linear layouts of complete graphs. In *Graph Drawing and Network Visualization - 29th International Symposium, GD 2021, Tübingen, Germany, September*

14-17, 2021, Revised Selected Papers (2021), H. C. Purchase and I. Rutter, Eds., vol. 12868 of *Lecture Notes in Computer Science*, Springer, pp. 257–270.

[18] Ganley, J. L., and Heath, L. S. The pagenumber of k-trees is o(k). *Discret. Appl. Math. 109*, 3 (2001), 215–221.

[19] Giacomo, E. D., and Meijer, H. Track drawings of graphs with constant queue number. In *Graph Drawing, 11th International Symposium, GD 2003, Perugia, Italy, September 21-24, 2003, Revised Papers* (2003), G. Liotta, Ed., vol. 2912 of *Lecture Notes in Computer Science*, Springer, pp. 214–225.

[20] Goldner, A., and Harary, F. Note on a smallest nonhamiltonian maximal planar graph. *Bull. Malaysian Math. Soc 6*, 1 (1975), 41–42.

[21] Heath, L. S. Embedding planar graphs in seven pages. In *25th Annual Symposium on Foundations of Computer Science, West Palm Beach, Florida, USA, 24-26 October 1984* (1984), IEEE Computer Society, pp. 74–83.

[22] Heath, L. S., Leighton, F. T., and Rosenberg, A. L. Comparing queues and stacks as mechanisms for laying out graphs. *SIAM J. Discrete Math. 5*, 3 (1992), 398–412.

[23] Heath, L. S., and Rosenberg, A. L. Laying out graphs using queues. *SIAM J. Comput. 21*, 5 (1992), 927–958.

[24] Hoffmann, M., and Klemz, B. Triconnected planar graphs of maximum degree five are subhamiltonian. In *27th Annual European Symposium on Algorithms, ESA 2019, September 9-11, 2019, Munich/Garching, Germany* (2019), M. A. Bender, O. Svensson, and G. Herman, Eds., vol. 144 of *LIPIcs*, Schloss Dagstuhl - Leibniz-Zentrum für Informatik, pp. 58:1–58:14.

[25] Jungeblut, P., Merker, L., and Ueckerdt, T. A sublinear bound on the page number of upward planar graphs. In *Proceedings of the 2022 ACM-SIAM Symposium on Discrete Algorithms, SODA 2022, Virtual Conference / Alexandria, VA, USA, January 9 - 12, 2022* (2022), J. S. Naor and N. Buchbinder, Eds., SIAM, pp. 963–978.

[26] Muder, D. J., Weaver, M. L., and West, D. B. Pagenumber of complete bipartite graphs. *J. Graph Theory 12*, 4 (1988), 469–489.

[27] OLLMANN, T. On the book thicknesses of various graphs. In *Southeastern Conference on Combinatorics, Graph Theory and Computing* (1973), F. Hoffman, R. Levow, and R. Thomas, Eds., vol. VIII of *Congressus Numerantium*, p. 459.

[28] PEMMARJU, S. V. Exploring the powers of stacks and queues via graph layouts.

[29] RENGARAJAN, S., AND MADHAVAN, C. E. V. Stack and queue number of 2-trees. In *Computing and Combinatorics, First Annual International Conference, COCOON '95, Xi'an, China, August 24-26, 1995, Proceedings* (1995), D. Du and M. Li, Eds., vol. 959 of *Lecture Notes in Computer Science*, Springer, pp. 203–212.

[30] RIEGER, X. Deque-numbers of graphs. University of Tübingen, Bachelor Thesis, 2023.

[31] WIECHERT, V. On the queue-number of graphs with bounded tree-width. *CoRR abs/1608.06091* (2016).

[32] WIGDERSON, A. The complexity of the Hamiltonian circuit problem for maximal planar graphs. Tech. Rep. TR-298, EECS Department, Princeton University, 1982.

[33] WOLZ, J. Engineering linear layouts with SAT. University of Tübingen, Master Thesis, 2018.

[34] WOOD, D. R. Queue layouts, tree-width, and three-dimensional graph drawing. In *FST TCS 2002: Foundations of Software Technology and Theoretical Computer Science, 22nd Conference Kanpur, India, December 12-14, 2002, Proceedings* (2002), M. Agrawal and A. Seth, Eds., vol. 2556 of *Lecture Notes in Computer Science*, Springer, pp. 348–359.

[35] YANNAKAKIS, M. Four pages are necessary and sufficient for planar graphs (extended abstract). In *Proceedings of the 18th Annual ACM Symposium on Theory of Computing, May 28-30, 1986, Berkeley, California, USA* (1986), J. Hartmanis, Ed., ACM, pp. 104–108.

[36] YANNAKAKIS, M. Embedding planar graphs in four pages. *J. Comput. Syst. Sci. 38*, 1 (1989), 36–67.

[37] YANNAKAKIS, M. Planar graphs that need four pages. *J. Comb. Theory, Ser. B 145* (2020), 241–263.